UNITED STATES AIR FORCE

SUMMER RESEARCH PROGRAM -- 1995

SUMMER RESEARCH EXTENSION PROGRAM FINAL REPORTS

VOLUME 5

ARNOLD ENGINEERING DEVELOPMENT CENTER

FRANK J. SEILER RESEARCH LABORATORY

WILFORD HALL MEDICAL CENTER

RESEARCH & DEVELOPMENT LABORATORIES

5800 Uplander Way

Culver City, CA 90230-6608

Program Director, RDL
Gary Moore

Program Manager, AFOSR
Major David Hart

Program Manager, RDL
Scott Licoscos

Program Administrator, RDL
Gwendolyn Smith

Program Administrator
Johnetta Thompson

Submitted to:

AIR FORCE OFFICE OF SCIENTIFIC RESEARCH

Bolling Air Force Base

Washington, D.C.

December 1995

REPORT DOCUMENTATION PAGE

AFRL-SR-BL-TR-00-

0701

1. AGENCY USE ONLY (Leave blank)	2. REPORT DATE	3. REP
	May, 1996	

4. TITLE AND SUBTITLE
1995 Summer Research Program (SRP), Summer Research Extension Program (SREP), Final Report, Volume 5, Arnold Eng. Development Center (AEDC), Frank J. Seiler Research Laboratory (FJSRL), and Wilford Hall Medical Center (WHMC)

5. FUNDING NUMBERS
F49620-93-C-0063

6. AUTHOR(S)
Gary Moore

7. PERFORMING ORGANIZATION NAME(S) AND ADDRESS(ES)
Research & Development Laboratories (RDL)
5800 Uplander Way
Culver City, CA 90230-6608

8. PERFORMING ORGANIZATION REPORT NUMBER

9. SPONSORING/MONITORING AGENCY NAME(S) AND ADDRESS(ES)
Air Force Office of Scientific Research (AFOSR)
801 N. Randolph St.
Arlington, VA 22203-1977

10. SPONSORING/MONITORING AGENCY REPORT NUMBER

11. SUPPLEMENTARY NOTES

12a. DISTRIBUTION AVAILABILITY STATEMENT
Approved for Public Release

12b. DISTRIBUTION CODE

13. ABSTRACT *(Maximum 200 words)*
The United States Air Force Summer Research Program (SRP) is designed to introduce university, college, and technical institute faculty members to Air Force research. This is accomplished by the faculty members, graduate students, and high school students being selected on a nationally advertised competitive basis during the summer intersession period to perform research at Air Force Research Laboratory (AFRL) Technical Directorates and Air Force Air Logistics Centers (ALC). AFOSR also offers its research associates (faculty only) an opportunity, under the Summer Research Extension Program (SREP), to continue their AFOSR-sponsored research at their home institutions through the award of research grants. This volume consists of the SREP program background, management information, statistics, a listing of the participants, and the technical report for each participant of the SREP working at the Arnold Engineering Development Center (AEDC), Frank J Seiler Research Laboratory (FJSRL), and Wilford Hall Medical Center (WHMC).

14. SUBJECT TERMS
Air Force Research, Air Force, Engineering, Laboratories, Reports, Summer, Universities, Faculty, Graduate Student, High School Student

15. NUMBER OF PAGES

16. PRICE CODE

17. SECURITY CLASSIFICATION OF REPORT	18. SECURITY CLASSIFICATION OF THIS PAGE	19. SECURITY CLASSIFICATION OF ABSTRACT	20. LIMITATION OF ABSTRACT
Unclassified	Unclassified	Unclassified	UL

GENERAL INSTRUCTIONS FOR COMPLETING SF 298

The Report Documentation Page (RDP) is used in announcing and cataloging reports. It is important that this information be consistent with the rest of the report, particularly the cover and title page. Instructions for filling in each block of the form follow. It is important to ***stay within the lines*** to meet ***optical scanning requirements.***

Block 1. Agency Use Only *(Leave blank)*.

Block 2. Report Date. Full publication date including day, month, and year, if available (e.g. 1 Jan 88). Must cite at least the year.

Block 3. Type of Report and Dates Covered. State whether report is interim, final, etc. If applicable, enter inclusive report dates (e.g. 10 Jun 87 - 30 Jun 88).

Block 4. Title and Subtitle. A title is taken from the part of the report that provides the most meaningful and complete information. When a report is prepared in more than one volume, repeat the primary title, add volume number, and include subtitle for the specific volume. On classified documents enter the title classification in parentheses.

Block 5. Funding Numbers. To include contract and grant numbers; may include program element number(s), project number(s), task number(s), and work unit number(s). Use the following labels:

C - Contract	**PR** - Project
G - Grant	**TA** - Task
PE - Program Element	**WU** - Work Unit Accession No.

Block 6. Author(s). Name(s) of person(s) responsible for writing the report, performing the research, or credited with the content of the report. If editor or compiler, this should follow the name(s).

Block 7. Performing Organization Name(s) and Address(es). Self-explanatory.

Block 8. Performing Organization Report Number. Enter the unique alphanumeric report number(s) assigned by the organization performing the report.

Block 9. Sponsoring/Monitoring Agency Name(s) and Address(es). Self-explanatory.

Block 10. Sponsoring/Monitoring Agency Report Number. *(If known)*

Block 11. Supplementary Notes. Enter information not included elsewhere such as: Prepared in cooperation with....; Trans. of....; To be published in.... When a report is revised, include a statement whether the new report supersedes or supplements the older report.

Block 12a. Distribution/Availability Statement. Denotes public availability or limitations. Cite any availability to the public. Enter additional limitations or special markings in all capitals (e.g. NOFORN, REL, ITAR).

DOD - See DoDD 5230.24, "Distribution Statements on Technical Documents."
DOE - See authorities.
NASA - See Handbook NHB 2200.2.
NTIS - Leave blank.

Block 12b. Distribution Code.

DOD - Leave blank.
DOE - Enter DOE distribution categories from the Standard Distribution for Unclassified Scientific and Technical Reports.
NASA - Leave blank.
NTIS - Leave blank.

Block 13. Abstract. Include a brief *(Maximum 200 words)* factual summary of the most significant information contained in the report.

Block 14. Subject Terms. Keywords or phrases identifying major subjects in the report.

Block 15. Number of Pages. Enter the total number of pages.

Block 16. Price Code. Enter appropriate price code *(NTIS only)*.

Blocks 17. - 19. Security Classifications. Self- explanatory. Enter U.S. Security Classification in accordance with U.S. Security Regulations (i.e., UNCLASSIFIED). If form contains classified information, stamp classification on the top and bottom of the page.

Block 20. Limitation of Abstract. This block must be completed to assign a limitation to the abstract. Enter either UL (unlimited) or SAR (same as report). An entry in this block is necessary if the abstract is to be limited. If blank, the abstract is assumed to be unlimited.

PREFACE

This volume is part of a five-volume set that summarizes the research of participants in the 1995 AFOSR Summer Research Extension Program (SREP). The current volume, Volume 1 of 5, presents the final reports of SREP participants at Armstrong Laboratory, Phillips Laboratory, Rome Laboratory, Wright Laboratory, Arnold Engineering Development Center, Frank J. Seiler Research Laboratory, and Wilford Hall Medical Center.

Reports presented in this volume are arranged alphabetically by author and are numbered consecutively -- e.g., 1-1, 1-2, 1-3; 2-1, 2-2, 2-3, with each series of reports preceded by a management summary. Reports in the five-volume set are organized as follows:

VOLUME	TITLE
1A	Armstrong Laboratory (part one)
1B	Armstrong Laboratory (part two)
2	Phillips Laboratory
3	Rome Laboratory
4A	Wright Laboratory (part one)
4B	Wright Laboratory (part two)
5	Arnold Engineering Development Center Frank J. Seiler Research Laboratory Wilford Hall Medical Center

1995 SREP FINAL REPORTS

Armstrong Laboratory

VOLUME 1

Report #	Report Title Author's University	Report Author
1	Determination of the Redox Capacity of Soil Sediment and Prediction of Pollutant University of Georgia, Athens, GA	Dr. James Anderson Analytical Chemistry AL/EQ
2	Finite Element Modeling of the Human Neck and Its Validation for the ATB Villanova University, Villanova, PA	Dr. Hashem Ashrafiuon Mechanical Engineering AL/CF
3	An Examination of the Validity of the Experimental Air Force ASVAB Composites Tulane University, New Orleans, LA	Dr. Michael Burke Psychology AL/HR
4	Fuel Identification by Neural Networks Analysis of the Response of Vapor Sensitive Sensors Arrays Edinboro University of Pennsylvania, Edinboro, PA	Dr. Paul Edwards Chemistry AL/EQ
5	A Comparison of Multistep vs Singlestep Arrhenius Integral Models for Describing Laser Induced Thermal Damage Florida International University, Miami, FL	Dr. Bernard Gerstman Physics AL/OE
6	Effects of Mental Workload and Electronic Support on Negotiation Performance University of Dayton, Dayton, OH	Dr. Kenneth Graetz Psychology AL/HR
7	Regression to the Mean in Half Life Studies University of Main, Orono, ME	Dr. Pushpa Gupta Mathematics & Statistics AL/AO
8	Application of the MT3D Solute Transport Model to the Made-2 Site: Calibration Florida State University, Tallahassee, FL	Dr. Manfred Koch Geophysics AL/EQ
9	Computer Calculations of Gas-Phase Reaction Rate Constants Florida State University, Tallahassee, FL	Dr. Mark Novotny SupercompComp. Res. I AL/EQ
10	Surface Fitting Three Dimensional Human Scan Data Ohio University, Athens, OH	Dr. Joseph Nurre Mechanical Engineering AL/CF
11	The Effects of Hyperbaric Oxygenation on Metabolism of Drugs and Other Xenobioti University of So. Carolina, Columbia, So. Carolina	Dr. Edward Piepmeier Pharmaceutics AL/AO
12	Maintaining Skills After Training: The Role of Opportunity to Perform Trained Tasks on Training Effectiveness Rice University, Houston, TX	Dr. Miguel Quinones Psychology AL/HR

1995 SREP FINAL REPORTS

Armstrong Laboratory

VOLUME 1 (cont.)

Report #	Report Title Author's University	Report Author
13	Nonlinear Transcutaneous Electrical Stimulation of the Vestibular System University of Illinois Urbana-Champaign, Urbana,IL	Dr. Gary Riccio Psychology AL/CF
14	Documentation of Separating and Separated Boundary Layer Flow, For Application Texas A&M University, College Station, TX	Dr. Wayne Shebilske Psychology AL/HR
15	Tactile Feedback for Simulation of Object Shape and Textural Information in Haptic Displays Ohio State University, Columbus, OH	Dr. Janet Weisenberger Speech & Hearing AL/CF
16	Melatonin Induced Prophylactic Sleep as a Countermeasure for Sleep Deprivation Oregon Health Sciences University, Portland, OR	Mr. Rod Hughes Psychology AL/CF

1995 SREP FINAL REPORTS

Phillips Laboratory

VOLUME 2A

Report #	Report Title Author's University	Report Author
1	Investigation of the Mixed-Mode Fracture Behavior of Solid Propellants University of Houston, Houston, TX	Dr. K. Ravi-Chandar Aeronautics PL/RK
2	Performance Study of ATM-Satellite Network SUNY-Buffalo, Buffalo, NY	Dr. Nasser Ashgriz Mechanical Engineering PL/RK
3	Characterization of CMOS Circuits Using a Highly Calibrated Low-Energy X-Ray Source Embry-Riddle Aeronautical Univ., Prescott, AZ	Dr. Raymond Bellem Computer Science PL/VT
4	Neutron Diagnostics for Pulsed Plasmas of Compact Toroid-Marauder Type Stevens Institute of Tech, Hoboken, NJ	Dr. Jan Brzosko Nuclear Physics PL/WS
5	Parallel Computation of Zernike Aberration Coefficients for Optical Aberration Correction University of Houston-Victoria, Victoria, TX	Dr. Meledath Damodaran Math & Computer Science PL/LI
6	Quality Factor Evaluation of Complex Cavities University of Denver, Denver, CO	Dr. Ronald DeLyser Electrical Engineering PL/WS
7	Unidirectional Ring Lasers and Laser Gyros with Multiple Quantum Well Gain University of New Mexico, Albuquerque, NM	Dr. Jean-Claude Diels Physics PL/LI
8	A Tool for the Formation of Variable Parameter Inverse Synthetic Aperture Radar University of Nevada, Reno, NV	Dr. James Henson Electrical Engineering PL/WS
9	Radar Ambiguity Functionals Univ. of Massachusetts at Lowell, Lowell, MA	Dr. Gerald Kaiser Physics PL/GP
10	The Synthesis and Chemistry of Peroxonitrites Peroxonitrous Acid Univ. of Massachusetts at Lowell, Lowell, MA	Dr. Albert Kowalak Chemistry PL/GP
11	Temperature and Pressure Dependence of the Band Gaps and Band Offsets University of Houston, Houston, TX	Dr. Kevin Malloy Electrical Engineering PL/VT
12	Theoretical Studies of the Performance of Novel Fiber-Coupled Imaging Interferom University of New Mexico, Albuquerque, NM	Dr. Sudhakar Prasad Physics PL/LI

1995 SREP FINAL REPORTS

Phillips Laboratory

VOLUME 2B

Report #	Author's University	Report Author
13	Static and Dynamic Graph Embedding for Parallel Programming Texas AandM Univ.-Kingsville, Kingsville, TX	Dr. Mark Purtill Mathematics PL/WS
14	Ultrafast Process and Modulation in Iodine Lasers University of New Mexico, Albuquerque, NM	Dr. W. Rudolph Physics PL/LI
15	Impedance Matching and Reflection Minimization for Transient EM Pulses Through University of New Mexico, Albuquerque, NM	Dr. Alexander Stone Mathematics and Statics PL/WS
16	Low Power Retromodular Based Optical Transceiver for Satellite Communications Utah State University, Logan, UT	Dr. Charles Swenson Electrical Engineering PL/VT
17	Improved Methods of Tilt Measurement for Extended Images in the Presence of Atmospheric Disturbances Using Optical Flow Michigan Technological Univ., Houghton, MI	Mr. John Lipp Electrical Engineering PL/LI
18	Thermoluminescence of Simple Species in Molecular Hydrogen Matrices Cal State Univ.-Northridge, Northridge, CA	Ms. Janet Petroski Chemistry PL/RK
19	Design, Fabrication, Intelligent Cure, Testing, and Flight Qualification University of Cincinnati, Cincinnati, OH	Mr. Richard Salasovich Mechanical Engineering PL/VT

1995 SREP FINAL REPORTS

Rome Laboratory

VOLUME 3

Report #	Author's University	Report Author
1	Performance Study of an ATM/Satellite Network Florida Atlantic University, Boca Raton, FL	Dr. Valentine Aalo Electrical Engineering RL/C3
2	Interference Excision in Spread Spectrum Communication Systems Using Time-Frequency Distributions Villanova University, Villanova, PA	Dr. Moeness Amin Electrical Engineering RL/C3
3	Designing Software by Reformulation Using KIDS Oklahoma State University, Stillwater, OK	Dr. David Benjamin Computer Science RL/C3
4	Detection Performance of Over Resolved Targets with Non-Uniform and Non-Gaussian Howard University, Washington, DC	Dr. Ajit Choudhury Engineering RL/OC
5	Computer-Aided-Design Program for Solderless Coupling Between Microstrip and Stripline Structures Southern Illinois University, Carbondale, IL	Dr. Frances Harackiewicz Electrical Engineering RL/ER
6	Spanish Dialect Identification Project Colorado State University, Fort Collins, CO	Dr. Beth Losiewicz Psycholinguistics RL/IR
7	Automatic Image Registration Using Digital Terrain Elevation Data University of Maine, Orono, ME	Dr. Mohamed Musavi Engineering RL/IR
8	Infrared Images of Electromagnetic Fields University of Colorado, Colorado Springs, CO	Dr. John Norgard Engineering RL/ER
9	Femtosecond Pump-Probe Spectroscopy System SUNY Institute of Technology, Utica, NY	Dr. Dean Richardson Photonics RL/OC
10	Synthesis and Properties B-Diketonate-Modified Heterobimetallic Alkoxides Tufts University, Medford, MA	Dr. Daniel Ryder, Jr. Chemical Engineering RL/ER
11	Optoelectronic Study of Seniconductor Surfaces and Interfaces Rensselaer Polytechnic Institute, Troy, NY	Dr. Xi-Cheng Zhang Physics RL/ER

1995 SREP FINAL REPORTS

Wright Laboratory

VOLUME 4A

Report #	Author's University	Report Author
1	An Investigation of the Heating and Temperature Distribution in Electrically Excited Foils Auburn University, Auburn, AL	Dr. Michael Baginski Electrical Engineering WL/MN
2	Micromechanics of Creep in Metals and Ceramics at High Temperature Wayne State University, Detroit, MI	Dr. Victor Berdichevsky Aerospace Engineering WL/FI
3	Development of a Fluorescence-Based Chemical Sensor for Simultaneous Oxygen Quantitation and Temp. Measurement Columbus College, Columbus, GA	Dr. Steven Buckner Chemistry WL/PO
4	Development of High-Performance Active Dynamometer Sys. for Machines and Drive Clarkson University, Potsdam, NY	Dr. James Carroll Electrical Engineering WL/PO
5	SOLVING $z(t)=1n[A\cos(w_1t)+B\cos(w_2)+C]$ Transylvania University, Lexington, KY	Dr. David Choate Mathematics WL/AA
6	Synthesis, Processing and Characterization of Nonlinear Optical Polymer Thin Films University of cincinnati, Cincinnati, OH	Dr. Stephen Clarson Matls Science& Engineering WL/ML
7	An Investigation of Planning and Scheduling Algorithms for Sensor Management Embry-Riddle Aeronautical University, Prescott, AZ	Dr. Milton Cone Comp. Science & Engineering WL/AA
8	A Study to Determine Wave Gun Firing Cycles for High Performance Model Launches Louisiana State University, Baton Rouge, LA	Dr. Robert Courter Mechanical Engineering WL/MN
9	Characterization of Electro-Optic Polymers University of Dayton, Dayton, OH	Dr. Vincent Dominic Electro Optics Program WL/ML
10	A Methodology for Affordability in the Design Process Clemson Univeristy, Clemson, SC	Dr. Georges Fadel Mechanical Engineering WL/MT
11	Data Reduction and Analysis for Laser Doppler Velocimetry North Carolina State University, Raleigh, NC	Dr. Richard Gould Mechanical Engineering WL/PO

1995 SREP FINAL REPORTS

Wright Laboratory

VOLUME 4A (cont.)

Report #	Author's University	Report Author
12	Hyperspectral Target Identification Using Bomen Spectrometer Data University of Dayton, Dayton, OH	Dr. Russell Hardie Electrical Engineering WL/AA
13	Robust Fault Detection and Classification Auburn University, Auburn, AL	Dr. Alan Hodel Electrical Engineering WL/MN
14	Multidimensional Algorithm Development and Analysis Mississippi State University, Mississippi State University, MS	Dr. Jonathan Janus Aerospace Engineering WL/MN
15	Characterization of Interfaces in Metal-Matrix Composites Michigan State University, East Lansing, MI	Dr. Iwona Jasiuk Materials Science WL/ML
16	TSI Mitigation: A Mountaintop Database Study Lafayette College, Easton, PA	Dr. Ismail Jouny Electrical Engineering WL/AA
17	Comparative Study and Performance Analysis of High Resolution SAR Imaging Techniques University of Florida, Gainesville, FL	Dr. Jian Li Electrical Engineering WL/AA

1995 SREP FINAL REPORTS

Wright Laboratory

VOLUME 4B

Report #	Author's University	Report Author
18	Prediction of Missile Trajectory University of Missouri-Columbia, Columbia, MO	Dr. Chun-Shin Lin Electrical Engineering WL/FI
19	Three Dimensional Deformation Comparison Between Bias and Radial Aircraft Tires Cleveland State University, Cleveland, OH	Dr. Paul Lin Mechanical Engineering WL/FI
20	Investigation of A1GaAs/GaAs Heterojunctin Bipolar Transistor Reliability Based University of Central Florida, Orlando, FL	Dr. Juin Liou Electrical Engineering WL/EL
21	Thermophysical Invariants From LWIR Imagery for ATR University of Virginia, Charlottesville, VA	Dr. Nagaraj Nandhakumar Electrical Engineering WL/AA
22	Effect of Electromagnetic Environment on Array Signal Processing University of Dayton, Dayton, OH	Dr. Krishna Pasala Electrical Engineering WL/AA
23	Functional Decomposotion of Binary, Multiple-Valued, and Fuzzy Logic Portland State University, Portland, OR	Dr. Marek Perkowski Electrical Engineering WL/AA
24	Superresolution of Passive Millimeter-Wave Imaging Auburn University, Auburn, AL	Dr. Stanley Reeves Electrical Engineering WL/MN
25	Development of a Penetrator Optimizer University of Alabama, Tuscaloosa, AL	Dr. William Rule Engineering Science WL/MN
26	Heat Transfer for Turbine Blade Film Cooling with Free Stream Turbulence-Measurements and Predictions University of Dayton, Dayton, OH	Dr. John Schauer Mech. & Aerosp. Engineering WL/FI
27	Neural Network Identification and Control in Metal Forging University of Florida, Gainesville, FL	Dr. Carla Schwartz Electrical Engineering WL/FI
28	Documentation of Separating and Separated Boundary Layer Flow, for Application University of Minnesota, Minneapolis, MN	Dr. Terrence Simon Mechanical Engineering WL/PO
29	Transmission Electron Microscopy of Semiconductor Heterojunctions Carnegie Melon University, Pittsburgh, PA	Dr. Marek Skowronski Matls Science & Engineering WL/EL

1995 SREP FINAL REPORTS

Wright Laboratory

VOLUME 4B (cont.)

Report #	Author's University	Report Author
30	Parser in SWI-PROLOG Wright State University, Dayton, OH	Dr. K. Thirunarayan Computer Science WL/EL
31	Development of Qualitative Process Control Discovery Systems for Polymer Composite and Biological Materials University of California, Los Angeles, CA	Dr. Robert Trelease Anatomy & Cell Biology WL/ML
32	Improved Algorithm Development of Massively Parallel Epic Hydrocode in Cray T3D Massively Parallel Computer Florida Atlantic University, Boca Raton, FL	Dr. Chi-Tay Tsai Engineering Mechanics WL/MN
33	The Characterization of the Mechanical Properties of Materials in a Biaxial Stress Environment University of Kentucky, Lexington, KY	Dr. John Lewis Materials Science Engineering WL/MN

1995 SREP FINAL REPORTS

VOLUME 5

Report #	Author's University	Report Author
	Arnold Engineering Development Center	
1	Plant-Wide Preventive Maintenance and Monitoring Vanderbilt University	Mr. Theodore Bapty Electrical Engineering AEDC
	Frank J. Seiler Research Laboratory	
1	Block Copolymers at Inorganic Solid Surfaces Colorado School of Mines, Golden, CO	Dr. John Dorgan Chemical Engineering FJSRL
2	Non-Linear Optical Properties of Polyacetylenes and Related Barry University, Miami, FL	Dr. M. A. Jungbauer Chemistry FJSRL
3	Studies of Second Harmonic Generation in Glass Waveguides Allegheny College, Meadville, PA	Dr. David Statman Physics FJSRL
	Wilford Hall Medical Center	
1	Biochemical & Cell Physiological Aspects of Hyperthermia University of Miami, Coral Gables, FL	Dr. W. Drost-Hansen Chemistry WHMC

1995 SUMMER RESEARCH EXTENSION PROGRAM (SREP) MANAGEMENT REPORT

1.0 BACKGROUND

Under the provisions of Air Force Office of Scientific Research (AFOSR) contract F49620-90-C-0076, September 1990, Research & Development Laboratories (RDL), an 8(a) contractor in Culver City, CA, manages AFOSR's Summer Research Program. This report is issued in partial fulfillment of that contract (CLIN 0003AC).

The Summer Research Extension Program (SREP) is one of four programs AFOSR manages under the Summer Research Program. The Summer Faculty Research Program (SFRP) and the Graduate Student Research Program (GSRP) place college-level research associates in Air Force research laboratories around the United States for 8 to 12 weeks of research with Air Force scientists. The High School Apprenticeship Program (HSAP) is the fourth element of the Summer Research Program, allowing promising mathematics and science students to spend two months of their summer vacations working at Air Force laboratories within commuting distance from their homes.

SFRP associates and exceptional GSRP associates are encouraged, at the end of their summer tours, to write proposals to extend their summer research during the following calendar year at their home institutions. AFOSR provides funds adequate to pay for SREP subcontracts. In addition, AFOSR has traditionally provided further funding, when available, to pay for additional SREP proposals, including those submitted by associates from Historically Black Colleges and Universities (HBCUs) and Minority Institutions (MIs). Finally, laboratories may transfer internal funds to AFOSR to fund additional SREPs. Ultimately the laboratories inform RDL of their SREP choices, RDL gets AFOSR approval, and RDL forwards a subcontract to the institution where the SREP associate is employed. The subcontract (see Appendix 1 for a sample) cites the SREP associate as the principal investigator and requires submission of a report at the end of the subcontract period.

Institutions are encouraged to share costs of the SREP research, and many do so. The most common cost-sharing arrangement is reduction in the overhead, fringes, or administrative charges institutions would normally add on to the principal investigator's or research associate's labor. Some institutions also provide other support (e.g., computer run time, administrative assistance, facilities and equipment or research assistants) at reduced or no cost.

When RDL receives the signed subcontract, we fund the effort initially by providing 90% of the subcontract amount to the institution (normally $18,000 for a $20,000 SREP). When we receive the end-of-research report, we evaluate it administratively and send a copy to the laboratory for a technical evaluation. When the laboratory notifies us the SREP report is acceptable, we release the remaining funds to the institution.

2.0 THE 1995 SREP PROGRAM

SELECTION DATA: A total of 719 faculty members (SFRP Associates) and 286 graduate students (GSRP associates) applied to participate in the 1994 Summer Research Program. From these applicants 185 SFRPs and 121 GSRPs were selected. The education level of those selected was as follows:

1994 SRP Associates, by Degree			
SFRP		GSRP	
PHD	MS	MS	BS
179	6	52	69

Of the participants in the 1994 Summer Research Program 90 percent of SFRPs and 25 percent of GSRPs submitted proposals for the SREP. Ninety proposals from SFRPs and ten from GSRPs were selected for funding, which equates to a selection rate of 54% of the SFRP proposals and of 34% for GSRP proposals.

1995 SREP: Proposals Submitted vs. Proposals Selected			
	Summer 1994 Participants	Submitted SREP Proposals	SREPs Funded
SFRP	185	167	90
GSRP	121	29	10
TOTAL	306	196	100

The funding was provided as follows:

Contractual slots funded by AFOSR	75
Laboratory funded	14
Additional funding from AFOSR	11
Total	100

Six HBCU/MI associates from the 1994 summer program submitted SREP proposals; six were selected (none were lab-funded; all were funded by additional AFOSR funds).

Proposals Submitted and Selected, by Laboratory		
	Applied	Selected
Armstrong Laboratory	41	19
Arnold Engineering Development Center	12	4
Frank J. Seiler Research Laboratory	6	3
Phillips Laboratory	33	19
Rome Laboratory	31	13
Wilford Hall Medical Center	2	1
Wright Laboratory	62	37
TOTAL		

Note: Phillips Laboratory funded 3 SREPs; Wright Laboratory funded 11; and AFOSR funded 11 beyond its contractual 75.

The 306 1994 Summer Research Program participants represented 135 institutions.

Institutions Represented on the 1994 SRP and 1995 SREP		
Number of schools represented in the Summer 92 Program	Number of schools represented in submitted proposals	Number of schools represented in Funded Proposals
135	118	73

Forty schools had more than one participant submitting proposals.

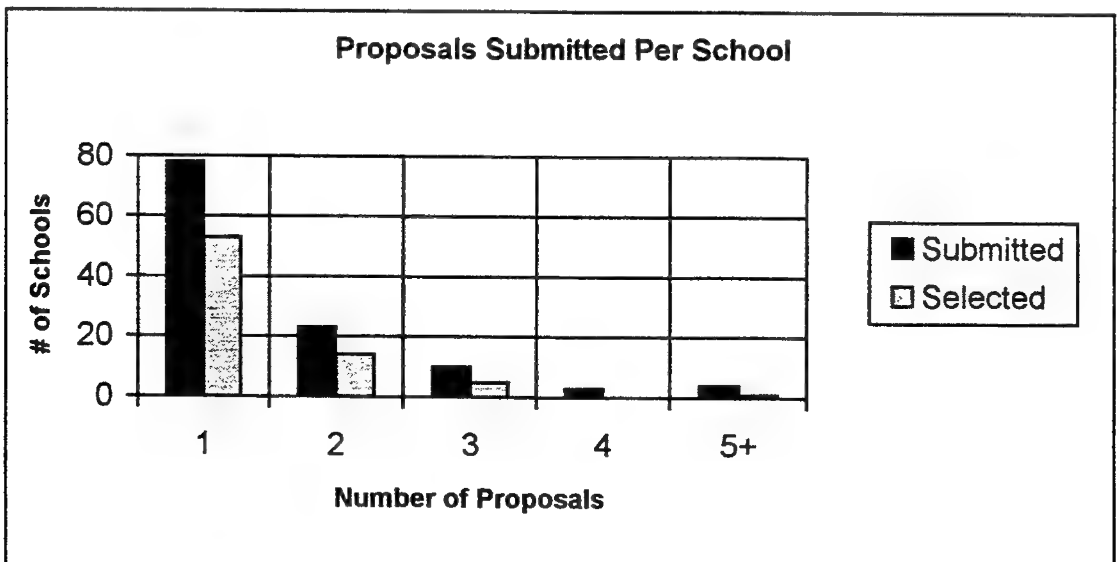

The selection rate for the 78 schools submitting 1 proposal (68%) was better than those submitting 2 proposals (61%), 3 proposals (50%), 4 proposals (0%) or 5+ proposals (25%). The 4 schools that submitted 5+ proposals accounted for 30 (15%) of the 196 proposals submitted.

Of the 196 proposals submitted, 159 offered institution cost sharing. Of the funded proposals which offered cost sharing, the minimum cost share was $1000.00, the maximum was $68,000.00 with an average cost share of $12,016.00.

Proposals and Institution Cost Sharing		
	Proposals Submitted	Proposals Funded
With cost sharing	159	82
Without cost sharing	37	18
Total	196	100

The SREP participants were residents of 41 different states. Number of states represented at each laboratory were:

States Represented, by Proposals Submitted/Selected per Laboratory		
	Proposals Submitted	Proposals Funded
Armstrong Laboratory	21	13
Arnold Engineering Development Center	5	2
Frank J. Seiler Research Laboratory	5	3
Phillips Laboratory	16	14
Rome Laboratory	14	7
Wilford Hall Medical Center	2	1
Wright Laboratory	24	20

Eleven of the 1995 SREP Principal Investigators also participated in the 1994 SREP.

ADMINISTRATIVE EVALUATION: The administrative quality of the SREP associates' final reports was satisfactory. Most complied with the formatting and other instructions provided to them by RDL. Ninety seven final reports and two interim reports have been received and are included in this report. The subcontracts were funded by $1,991,623.00 of Air Force money. Institution cost sharing totaled $985,353.00.

TECHNICAL EVALUATION: The form used for the technical evaluation is provided as Appendix 2. ninety-two evaluation reports were received. Participants by laboratory versus evaluations submitted is shown below:

	Participants	Evaluations	Percent
Armstrong Laboratory	23[1]	20	95.2
Arnold Engineering Development Center	4	4	100
Frank J. Seiler Research Laboratory	3	3	100
Phillips Laboratory	19[2]	18	100
Rome Laboratory	13	13	100
Wilford Hall Medical Center	1	1	100
Wright Laboratory	37	34	91.9
Total			

Notes:

1: Research on two of the final reports was incomplete as of press time so there aren't any technical evaluations on them to process, yet. Percent complete is based upon 20/21=95.2%

2: One technical evaluation was not completed because one of the final reports was incomplete as of press time. Percent complete is based upon 18/18=100%

3: See notes 1 and 2 above. Percent complete is based upon 93/97=95.9%

The number of evaluations submitted for the 1995 SREP (95.9%) shows a marked improvement over the 1994 SREP submittals (65%).

PROGRAM EVALUATION: Each laboratory focal point evaluated ten areas (see Appendix 2) with a rating from one (lowest) to five (highest). The distribution of ratings was as follows:

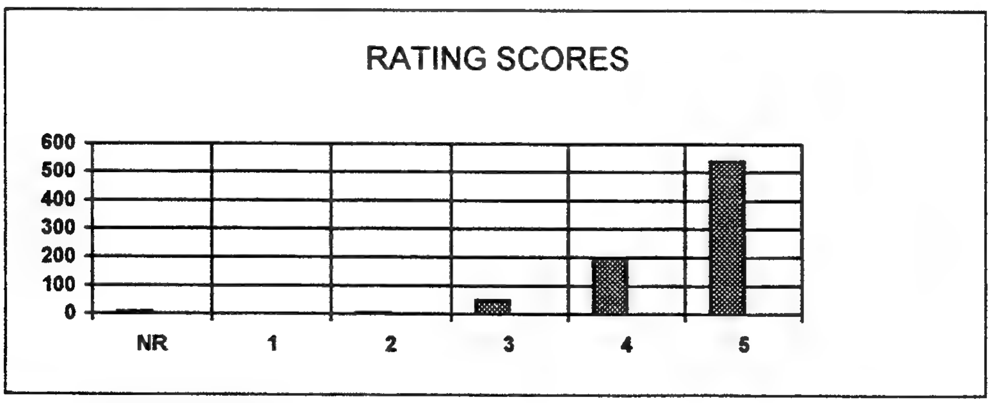

Rating	Not Rated	1	2	3	4	5
# Responses	7	1	7	62 (6%)	226 (25%)	617 (67%)

The 8 low ratings (one 1 and seven 2's) were for question 5 (one 2) "The USAF should continue to pursue the research in this SREP report" and question 10 (one 1 and six 2's) "The

one-year period for complete SREP research is about right", in addition over 30% of the threes (20 of 62) were for question ten. The average rating by question was:

Question	1	2	3	4	5	6	7	8	9	10
Average	4.6	4.6	4.7	4.7	4.6	4.7	4.8	4.5	4.6	4.0

The distribution of the averages was:

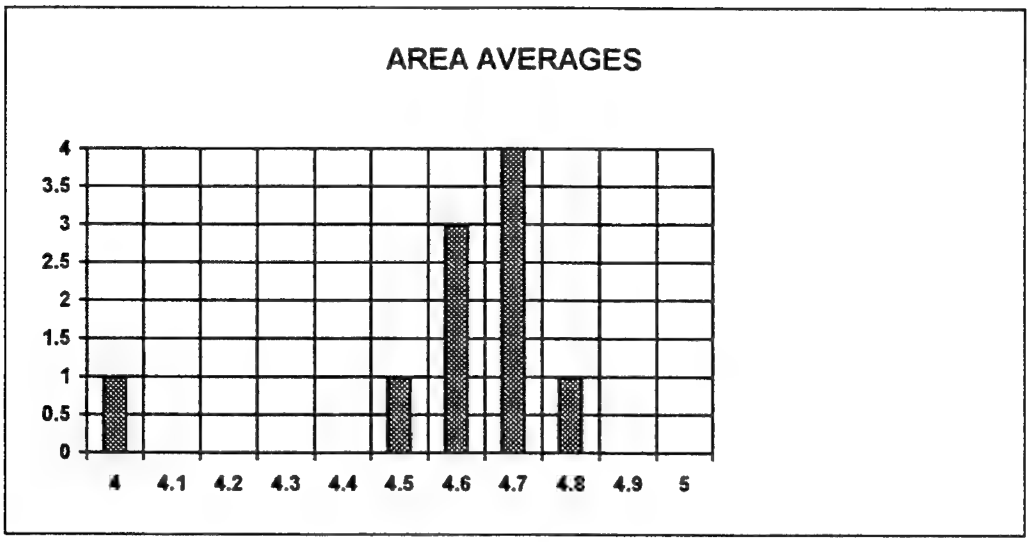

Area 10 "the one-year period for complete SREP research is about right" had the lowest average rating (4.1). The overall average across all factors was 4.6 with a small sample standard deviation of 0.2. The average rating for area 10 (4.1) is approximately three sigma lower than the overall average (4.6) indicating that a significant number of the evaluators feel that a period of other than one year should be available for complete SREP research.

The average ratings ranged from 3.4 to 5.0. The overall average for those reports that were evaluated was 4.6. Since the distribution of the ratings is not a normal distribution the average of 4.6 is misleading. In fact over half of the reports received an average rating of 4.8 or higher. The distribution of the average report ratings is as shown:

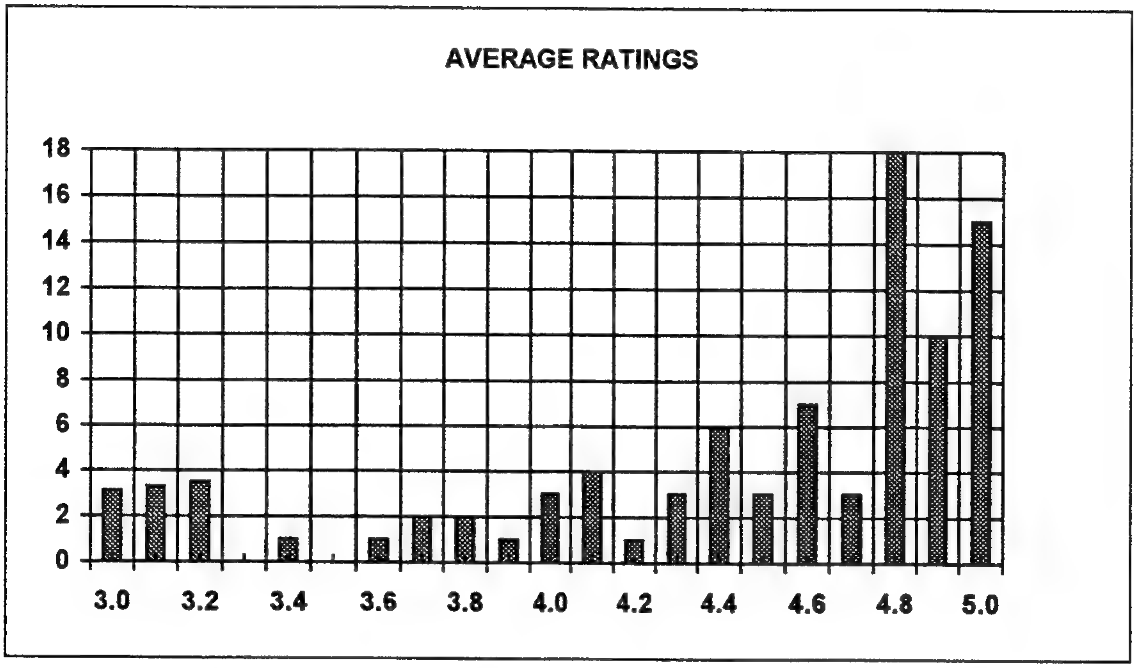

It is clear from the high ratings that the laboratories place a high value on AFOSR's Summer Research Extension Programs.

3.0 SUBCONTRACTS SUMMARY

Table 1 provides a summary of the SREP subcontracts. The individual reports are published in volumes as shown:

Laboratory	Volume
Armstrong Laboratory	1A, 1B
Arnold Engineering Development Center	5
Frank J. Seiler Research Laboratory	5
Phillips Laboratory	2
Rome Laboratory	3
Wilford Hall Medical Center	5
Wright Laboratory	4A, 4B

1995 SREP SUB-CONTRACT DATA

Report Author Author's University	Author's Degree	Sponsoring Lab	Performance Period		Contract Amount	Univ. Cost Share
Anderson , James **Analytical Chemistry** **University of Georgia, Athens, GA**	**PhD** 95-0807	**AL/EQ**	**01/01/95**	**12/31/95**	**$25000.00**	**$1826.00**
		Determination of the Redox Capacity of Soil Sediment and Prediction of Pollutant				
Ashrafiuon , Hashem **Mechanical Engineering** **Villanova University, Villanova, PA**	**PhD** 95-0800	**AL/CF**	**01/01/95**	**12/31/95**	**$25000.00**	**$19528.00**
		Finite Element Modeling of the Human Neck and Its Validation for the ATB Model				
Burke , Michael **Tulane University** **Tulane University, New Orleans, LA**	**PhD** 95-0811	**AL/HR**	**01/01/95**	**09/30/95**	**$25000.00**	**$1818.00**
		An Examination of the Validity of the New Air Force ASVAB Composites				
Edwards , Paul **Chemistry** **Edinboro Univ of Pennsylvania, Edinboro, PA**	**PhD** 95-0808	**AL/EQ**	**01/01/95**	**12/31/95**	**$25000.00**	**$5000.00**
		Fuel Identification by Neural Networks Analysis of the Response of Vapor Sensiti				
Gerstman , Bernard **Physics** **Florida International Universi, Miami, FL**	**PhD** 95-0815	**AL/OE**	**01/01/95**	**12/31/95**	**$24289.00**	**$2874.00**
		A Comparison of Multistep vs Singlestep Arrhenius Integral Models for Describing				
Graetz , Kenneth **Department of Psychology** **University of Dayton, Dayton, OH**	**PhD** 95-0812	**AL/HR**	**01/01/95**	**12/31/95**	**$25000.00**	**$0.00**
		Effects of Mental Workload and Electronic Support on Negotiation Performance				
Gupta , Pushpa **Mathematics** **University of Maine, Orono, ME**	**PhD** 95-0802	**AL/AO**	**01/01/95**	**12/31/95**	**$25000.00**	**$2859.00**
		Regression to the Mean in Half Life Studies				
Koch , Manfred **Geophysics** **Florida State University, Tallahassee, FL**	**PhD** 95-0809	**AL/EQ**	**12/01/94**	**04/30/95**	**$25000.00**	**$0.00**
		Application of the MT3D Solute Transport Model to the Made-2 Site: Calibration				
Novotny , Mark **Supercomputer Comp Res. I** **Florida State University, Tallahassee, FL**	**PhD** 95-0810	**AL/EQ**	**01/01/95**	**12/31/95**	**$25000.00**	**$0.00**
		Computer Calculations of Gas-Phase Reaction Rate Constants				
Nurre , Joseph **Mechanical Engineering** **Ohio University, Athens, OH**	**PhD** 95-0804	**AL/CF**	**01/01/95**	**12/31/95**	**$25000.00**	**$20550.00**
		Surface Fitting Three Dimensional Human Head Scan Data				
Piepmeier , Edward **Pharmaceutics** **University of South Carolina, Columbia, SC**	**PhD** 95-0801	**AL/AO**	**01/01/95**	**12/31/95**	**$25000.00**	**$11740.00**
		The Effects of Hyperbaric Oxygenation on Metabolism of Drugs and Other Xenobioti				
Quinones , Miguel **Psychology** **Rice University, Houston, TX**	**PhD** 95-0813	**AL/HR**	**01/01/95**	**12/31/95**	**$25000.00**	**$4000.00**
		Maintaining Skills After Training: The Role of Opportunity to Perform Trained T				
Riccio , Gary **Psychology** **Univ of IL Urbana-Champaign, Urbana, IL**	**PhD** 95-0806	**AL/CF**	**01/01/95**	**05/31/95**	**$22931.00**	**$0.00**
		Nonlinear Transcutaneous Electrical Stimulation of the Vestibular System				
Shebilske , Wayne **Dept of Psychology** **Texas A&M University, College Station, TX**	**PhD** 95-0814	**AL/HR**	**01/01/95**	**12/31/95**	**$25000.00**	**$5614.00**
		Cognitive Factors in Distr Training Effects During Acquisition of Complex Skills				

1995 SREP SUB-CONTRACT DATA

Report Author Author's University	Author's Degree	Sponsoring Lab	Performance Period	Contract Amount	Univ. Cost Share
Weisenberger , Janet Dept of Speech & Hearing Ohio State University, Columbus, OH	PhD 95-0805	AL/CF	01/01/95 12/31/95	$25000.00	$12234.00
		Tactile Feedback for Simulation of Object Shape and Textural Information in Hapt			
Hughes , Rod Psychology Oregon Health Sciences University, Portland, OR	MA 95-0803	AL/CF	01/01/95 12/31/95	$25000.00	$0.00
		Melatonin Induced Prophylactic Sleep as a Countermeasure for Sleep Deprivation			
Bapty , Theodore Electrical Engineering Vanderbilt University, Nashville, TN	MS 95-0848	AEDC/E	01/01/95 12/31/95	$24979.00	$0.00
		Plant-Wide Preventive Maintenance & Monitoring			
Dorgan , John Chemical Engineering Colorado School of Mines, Golden, CO	PhD 95-0834	FJSRL/F	01/01/95 12/31/95	$25000.00	$0.00
		Block Copolymers at Inorganic Solid Surfaces			
Jungbauer , Mary Ann Chemistry Barry University, Miami, FL	PhD 95-0836	FJSRL/F	01/01/95 12/31/95	$25000.00	$24714.00
		Non-Linear Optical Properties of Polyacetylenes and Related Substituted Compound			
Statman , David Physics Allegheny College, Meadville, PA	PhD 95-0835	FJSRL/F	01/01/95 12/31/95	$25000.00	$6500.00
		Studies of Second Harmonic Generation in Glass Waveguides			
, Krishnaswamy Aeronautics University of Houston, Houston, TX	PhD 95-0818	PL/RK	01/01/95 12/31/95	$24993.00	$8969.00
		Mixed-Mode Fracture of Solid Propellants			
Ashgriz , Nasser Mechanical Engineering SUNY-Buffalo, Buffalo, NY	PhD 95-0816	PL/RK	01/01/95 12/31/95	$25000.00	$22329.00
		Effects of the Jet Characteristics on the Atomization and Mixing in A Pair of Im			
Bellem , Raymond Computer Science Embry-Riddle Aeronautical Univ, Prescott, AZ	PhD 95-0817	PL/VT	12/01/94 11/30/95	$20000.00	$8293.00
		Experimental Studies of the Effects of Ionizing Radiation on Commerically Proces			
Brzosko , Jan Nuclear Physics Stevens Institute of Tech, Hoboken, NJ	PhD 95-0828	PL/WS	11/01/94 02/01/95	$24943.00	$0.00
		Neutron Diagnostics for Pulsed Plasmas of Compact Toroid - Marauder Type			
Damodaran , Meledath Math & Computer Science University of Houston-Victoria, Victoria, TX	PhD 95-0831	PL/LI	01/01/95 12/31/94	$24989.00	$9850.00
		Parallel Computation of Zernike Aberration Coefficients for Optical Aber Correct			
DeLyser , Ronald Electrical Engineering University of Denver, Denver, CO	PhD 95-0877	PL/WS	01/01/95 12/31/95	$25000.00	$46066.00
		Quality Factor Evaluation of Complex Cavities			
Diels , Jean-Claude Physics University of New Mexico, Albuquerque, NM	PhD 95-0819	PL/LI	01/01/95 12/31/95	$25000.00	$0.00
		Unidirectional Ring Lasers and Laseer Gyros with Multiple Quantum Well Gain Medi			
Henson , James Electrical Engineering University of Nevada, Reno, NV	PhD 95-0820	PL/WS	01/01/95 12/31/95	$25000.00	$0.00
		Automatic Feature Extraction and Assessment of Wideband Range-Doppler Imagery of			
Kaiser , Gerald Physics University of Mass/Lowell, Lowell, MA	PhD 95-0821	PL/GP	01/01/95 12/31/95	$25000.00	$5041.00
		Multiresolution Analysis with Physical Wavelets			

1995 SREP SUB-CONTRACT DATA

Report Author Author's University	Author's Degree	Sponsoring Lab	Performance Period		Contract Amount	Univ. Cost Share
Kowalak , Albert Chemistry University of Massachusetts/Lo, Lowell, MA	PhD 95-0822	PL/GP	01/01/95	12/31/95	$24996.00	$4038.00
		The Synthesis and Chemistry of Peroxonitrites and Peroxonitrous Acid				
Malloy , Kevin Electrical Engineering University of New Mexico, Albuquerque, NM	PhD 95-0829	PL/VT	01/01/95	12/31/95	$24999.00	$0.00
		Temperature & Pressure Dependence of the Band Gaps & Band Offsets				
Prasad , Sudhakar Physics University of New Mexico, Albuquerque, NM	PhD 95-0823	PL/LI	01/01/95	12/31/95	$25000.00	$11047.00
		Theoretical Studies of the Performance of Novel Fiber-Coupled Imaging Interferom				
Purtill , Mark Mathematics Texas A&M Univ-Kingsville, Kingsville, TX	PhD 95-0824	PL/WS	01/01/95	12/31/95	$25000.00	$100.00
		Static and Dynamic Graph Embedding for Parallel Programming				
Rudolph , Wolfgang Physics University of New Mexico, Albuquerque, NM	PhD 95-0833	PL/LI	01/01/95	12/31/95	$24982.00	$6000.00
		Ultrafast Process and Modulation in Iodine Lasers				
Stone , Alexander Mathematics & Statistics University of New Mexico, Alburquerque, NM	PhD 95-0827	PL/WS	01/01/95	12/31/95	$24969.00	$0.00
		Impedance Matching And Reflection Minimization For Transient EM Pulses Through D				
Swenson , Charles Dept of Electrical Engnr Utah State University, Logan, UT	PhD 95-0826	PL/VT	01/01/95	12/31/95	$25000.00	$25000.00
		Low Power Retromodulator based Optical Transceiver for Satellite Communications				
Lipp , John Electrical Engineering Michigan Technological Univ, Houghton, MI	MS 95-0832	PL/LI	01/01/95	12/31/95	$24340.00	$15200.00
		Improved Methods of Tilt Measurement for Extended Images in the Presence of Atmo				
Petroski , Janet Chemistry Cal State Univ/Northridge, Northridge, CA	BA 95-0830	PL/RK	10/01/94	12/31/94	$4279.00	$0.00
		Thermoluminescence of Simple Species in Molecular Hydrogen Matrices				
Salasovich , Richard Mechanical Engineering University of Cincinnati, Cincinnati, OH	MS 95-0825	PL/VT	01/01/95	12/31/95	$25000.00	$4094.00
		Design, Fabrication, Intelligent Cure, Testing, and Flight Qualification of an A				
Aalo , Valentine Dept of Electrical Engr Florida Atlantic University, Boca Raton, FL	PhD 95-0837	RL/C3	01/01/95	12/31/95	$25000.00	$13120.00
		Performance Study of an ATM/Satellite Network				
Amin , Moeness Electrical Engineering Villanova University, Villanova, PA	PhD 95-0838	RL/C3	01/01/95	12/31/95	$25000.00	$34000.00
		Interference Excision in Spread Spectrum Communication Systems Using Time-Freque				
Benjamin , David Computer Science Oklahoma State University, Stillwater, OK	PhD 95-0839	RL/C3	01/01/95	12/31/95	$24970.00	$0.00
		Designing Software by Decomposition using KIDS				
Choudhury , Ajit Engineering Howard University, Washington, DC	PhD 95-0840	RL/OC	11/30/94	10/31/95	$25000.00	$0.00
		Detection Performance of Over Resolved Targets with Non-Uniform and Non-GAussian				
Harackiewicz , Frances Electrical Engineering So. Illinois Univ-Carbondale, Carbondale, IL	PhD 95-0841	RL/ER	01/01/95	12/31/95	$23750.00	$29372.00
		Computer-Aided-Design Program for Solderless Coupling Between Microstrip and Str				

1995 SREP SUB-CONTRACT DATA

Report Author Author's University	Author's Degree	Sponsoring Lab	Performance Period		Contract Amount	Univ. Cost Share
Losiewicz , Beth Psycholinguistics Colorado State University, Fort Collins, CO	PhD 95-0842	RL/IR	01/01/95	12/31/95	$25000.00	$4850.00
		Spanish Dialect Identification Project				
Musavi , Mohamad University of Maine, Orono, ME	PhD 95-0843	RL/IR	01/01/95	12/31/95	$25000.00	$12473.00
		Automatic Image Registration Using Digital Terrain Elevation Data				
Norgard , John Elec & Comp Engineering Univ of Colorado-Colorado Sprg, Colorado	PhD 95-0844	RL/ER	01/01/95	12/31/95	$25000.00	$2500.00
		Infrared Images of Electromagnetic Fields				
Richardson , Dean Photonics SUNY Institute of Technology, Utica, NY	PhD 95-0845	RL/OC	01/01/95	12/31/95	$25000.00	$15000.00
		Femtosecond Pump-Probe Spectroscopy System				
Ryder, Jr. , Daniel Chemical Engineering Tufts University, Medford, MA	PhD 95-0846	RL/ER	01/01/95	12/31/95	$25000.00	$0.00
		Synthesis and Properties B-Diketonate-Modified Heterobimetallic Alkoxides				
Zhang , Xi-Cheng Physics Rensselaer Polytechnic Institu, Troy, NY	PhD 95-0847	RL/ER	01/01/95	12/31/95	$25000.00	$0.00
		Optoelectronic Study of Seniconductor Surfaces and Interfaces				
Drost-Hansen , Walter Chemistry University of Miami, Coral Gables, FL	PhD 95-0875	WHMC/	01/01/95	12/31/95	$25000.00	$8525.00
		Biochemical & Cell Physiological Aspects of Hyperthermia				
Baginski , Michael Electrical Engineering Auburn University, Auburn, AL	PhD 95-0869	WL/MN	01/01/95	12/31/95	$24995.00	$10098.00
		An Investigation of the Heating and Temperature Distribution in Electrically Exc				
Berdichevsky , Victor Aerospace Engineering Wayne State University, Detroit, MI	PhD 95-0849	WL/FI	01/01/95	12/31/95	$25000.00	$0.00
		Micromechanics of Creep in Metals and Ceramics at High Temperature				
Buckner , Steven Chemistry Colullmbus College, Columbus, GA	PhD 95-0850	WL/PO	01/01/95	12/31/95	$24900.00	$8500.00
		Development of a Fluorescenece-Based Chemical Sensor for Simultaneous Oxygen Qua				
Carroll , James Electrical Engineering Clarkson University, Potsdam, NY	PhD 95-0881	WL/PO	01/01/95	12/31/95	$24944.00	$38964.00
		Development of HIgh-Performance Active Dynamometer System for Machines and Drive				
Choate , David Mathematics Transylvania University, Lexington, KY	PhD 95-0851	WL/AA	01/01/95	12/31/95	$24993.00	$8637.00
		SOLVING z(t)=ln{/A[cos(w1t)]+B[sin(w2t)]+C}				
Clarson , Stephen Materials Sci & Eng University of Cincinnati, Cincinnati, OH	PhD 95-0852	WL/ML	12/01/94	11/30/95	$25000.00	$15000.00
		Synthesis, Processing and Characterization of Nonlinear Optical Polymer Thin Fil				
Cone , Milton Comp Science & Elec Eng Embry-Riddel Aeronautical Univ, Prescott, AZ	PhD 95-0853	WL/AA	01/01/95	12/31/95	$25000.00	$11247.00
		An Investigation of Planning and Scheduling Algorithms for Sensor Management				
Courter , Robert Mechanical Engineering Louisiana State University, Baton Rouge, LA	PhD 95-0854	WL/MN	01/01/95	12/31/95	$25000.00	$3729.00
		A Study to Determine Wave Gun Firing Cycles for High Performance Model Launches				

1995 SREP SUB-CONTRACT DATA

Report Author Author's University	Author's Degree	Sponsoring Lab	Performance Period	Contract Amount	Univ. Cost Share
Dominic , Vincent Electro Optics Program University of Dayton, Dayton, OH	PhD 95-0868	WL/ML Characterization of Electro-Optic Polymers	01/01/95 12/31/95	$25000.00	$12029.00
Fadel , Georges Dept of Mechanical Engnr Clemson University, Clemson, SC	PhD 95-0855	WL/MT A Methodology for Affordability in the Design Process	01/01/95 12/31/95	$25000.00	$8645.00
Gould , Richard Mechanical Engineering North Carolina State Univ, Raleigh, NC	PhD 95-0856	WL/PO Data Reduction and Analysis for laser Doppler Velocimetry	01/01/95 12/31/95	$24998.00	$9783.00
Hardie , Russell Electrical Engineering Univsity of Dayton, Dayton, OH	PhD 95-0882	WL/AA Hyperspectral Target Identification Using Bomen Spectometer Data	01/01/95 12/31/95	$24999.00	$7415.00
Hodel , Alan Electrical Engineering Auburn University, Auburn, AL	PhD 95-0870	WL/MN Robust Falut Tolerant Control: Fault Detection and Classification	01/01/95 12/31/95	$24990.00	$9291.00
Janus , Jonathan Aerospace Engineering Mississippi State University, Mississippi State,	PhD 95-0871	WL/MN Multidimensional Algorithm Development & Analysis	01/01/95 12/31/95	$25000.00	$7143.00
Jasiuk , Iwona Dept of Materials Science Michigan State University, East Lansing, MI	PhD 95-0857	WL/ML Characterization of Interfaces in Metal-Matrix Composites	01/01/95 12/31/95	$25000.00	$0.00
Jouny , Ismail Electrical Engineering Lafayette College, Easton, PA	PhD 95-0880	WL/AA TSI Mitigation: A Mountaintop Database Study	01/01/95 12/31/95	$24300.00	$5200.00
Li , Jian Electrical Engineering University of Florida, Gainesville, FL	PhD 95-0859	WL/AA Comparative Study and Performance Analysis of High Resolution SAR Imaging Techni	10/10/95 12/31/95	$25000.00	$4000.00
Lin , Chun-Shin Electrical Engineering University of Missouri-Columbi, Columbia, MO	PhD 95-0883	WL/FI Prediction of Missile Trajectory	01/01/95 12/31/95	$25000.00	$2057.00
Lin , Paul Mechanical Engineering Cleveland State University, Cleveland, OH	PhD 95-0860	WL/FI Three Dimensional Deformation Comparison Between Bias and Radial Aircraft Tires	01/01/95 12/31/95	$25000.00	$6886.00
Liou , Juin Electrical Engineering University of Central Florida, Orlando, FL	PhD 95-0876	WL/EL Investigation of AlGaAs/GaAs Heterojunction Bipolar Transister Reliability Based	01/01/95 12/31/95	$25000.00	$11040.00
Nandhakumar , Nagaraj Electrical Engineering University of Virginia, Charlottesville, VA	PhD 95-0861	WL/AA Thermophysical Invariants fro, LWIR Imagery for ATR	01/01/95 12/31/95	$24979.00	$4500.00
Pasala , Krishna Dept of Electrical Engr University of Dayton, Dayton, OH	PhD 95-0879	WL/AA Effect of Electromagmetic Enviornment on Array Signal Processing	01/01/95 12/31/95	$25000.00	$1078.00
Perkowski , Marek Dept of Electrical Engnr Portland State University, Portland, OR	PhD 95-0878	WL/AA Functional Decomposition of Binary,Multiple-Valued, & Fuzzy Logic	01/01/95 09/15/95	$24947.00	$18319.00

1995 SREP SUB-CONTRACT DATA

Report Author Author's University	Author's Degree	Sponsoring Lab	Performance Period		Contract Amount	Univ. Cost Share
Reeves , Stanley Dept of Electrical Engnr Auburn University, Auburn, AL	PhD 95-0862	WL/MN	01/01/95	12/31/95	$25000.00	$0.00
		Superresolution of Passive Millimeter-Wave Imaging				
Rule , William Engineering Mechanics University of Alabama, Tuscaloosa, AL	PhD 95-0872	WL/MN	01/01/95	12/31/95	$24968.00	$14576.00
		Development of a Penetrator Optimizer				
Schauer , John Mech & Aerosp Eng University of Dayton, Dayton, OH	PhD 95-0873	WL/PO	11/01/94	11/30/95	$25000.00	$7428.00
		Heat Transfer for Turbine Blade Film Cooling with Free Stream Turbulence - Measu				
Schwartz , Carla Electrical Engineering University of Florida, Gainesville, FL	PhD 95-0863	WL/FI	01/01/95	12/31/95	$25000.00	$0.00
		Neural Network Identification and Control in Metal Forging				
Simon , Terrence Dept of Mechanical Engineering University of Minnesota, Minneapolis, MN	PhD 95-0864	WL/PO	01/01/95	12/31/95	$24966.00	$3996.00
		Documentation of Separating and Separated Boundary Layer Flow, for Application				
Skowronski , Marek Solid State Physics Carnegie Melon University, Pittsburgh, PA	PhD 95-0865	WL/EL	01/01/95	12/31/95	$25000.00	$6829.00
		Transmission Electron Microscopy of Semiconductor Heterojunctions				
Thirunarayan , Krishnaprasad Computer Science Wright State University, Dayton, OH	PhD 95-0866	WL/EL	01/01/95	12/31/95	$25000.00	$2816.00
		VHDL-93 Parser in SWI-PROLOG: A Basis for Design Query System				
Trelease , Robert Dept of Anatomy & Cell Bi University of California, Los Angeles, CA	PhD 95-0867	WL/ML	12/01/94	12/01/95	$25000.00	$0.00
		Development of Qualitative Process Control Discovery Systems for Polymar Composi				
Tsai , Chi-Tay Engineering Mechanics Florida Atlantic University, Boca Raton, FL	PhD 95-0874	WL/MN	01/01/95	12/31/95	$24980.00	$0.00
		Improved Algorithm Development of Massively Parallel Epic Hydrocode in Cray T3D				
Lewis , John Materials Science Engrng University of Kentucky, Lexington, KY	MS 95-0858	WL/MN	01/01/95	12/31/95	$25000.00	$13833.00
		The Characterization of the Mechanical Properties of Materials in a Biaxial Stre				

APPENDIX 1:

SAMPLE SREP SUBCONTRACT

AIR FORCE OFFICE OF SCIENTIFIC RESEARCH
1995 SUMMER RESEARCH EXTENSION PROGRAM
SUBCONTRACT 95-0837

BETWEEN

Research & Development Laboratories
5800 Uplander Way
Culver City, CA 90230-6608

AND

Florida Atlantic University
Department of Electrical Engineering
Boca Raton, FL 33431

REFERENCE: Summer Research Extension Program Proposal 95-0837
Start Date: 01-01-95 End Date: 12-31-95
Proposal Amount: $25,000.00

(1) PRINCIPAL INVESTIGATOR: Dr. Valentine A. Aalo
Department of Electrical Engineering
Florida Atlantic University
Boca Raton, FL 33431

(2) UNITED STATES AFOSR CONTRACT NUMBER: F49620-93-C-0063

(3) CATALOG OF FEDERAL DOMESTIC ASSISTANCE NUMBER (CFDA):12.800
PROJECT TITLE: AIR FORCE DEFENSE RESEARCH SOURCES PROGRAM

(4) ATTACHMENT 1 REPORT OF INVENTIONS AND SUBCONTRAACT
2 CONTRACT CLAUSES
3 FINAL REPORT INSTRUCTIONS

*****SIGN SREP SUBCONTRACT AND RETURN TO RDL*****

1. <u>BACKGROUND:</u> Research & Development Laboratories (RDL) is under contract (F49620-93-C-0063) to the United States Air Force to administer the Summer Research Program (SRP), sponsored by the Air Force Office of Scientific Research (AFOSR), Bolling Air Force Base, D.C. Under the SRP, a selected number of college faculty members and graduate students spend part of the summer conducting research in Air Force laboratories. After completion of the summer tour participants may submit, through their home institutions, proposals for follow-on research. The follow-on research is known as the Summer Research Extension Program (SREP). Approximately 61 SREP proposals annually will be selected by the Air Force for funding of up to $25,000; shared funding by the academic institution is encouraged. SREP efforts selected for funding are administered by RDL through subcontracts with the institutions. This subcontract represents an agreement between RDL and the institution herein designated in Section 5 below.

2. <u>RDL PAYMENTS:</u> RDL will provide the following payments to SREP institutions:

   - 80 percent of the negotiated SREP dollar amount at the start of the SREP research period.
   - The remainder of the funds within 30 days after receipt at RDL of the acceptable written final report for the SREP research.

3. <u>INSTITUTION'S RESPONSIBILITIES:</u> As a subcontractor to RDL, the institution designated on the title page will:

a. Assure that the research performed and the resources utilized adhere to those defined in the SREP proposal.

b. Provide the level and amounts of institutional support specified in the SREP proposal..

c. Notify RDL as soon as possible, but not later than 30 days, of any changes in 3a or 3b above, or any change to the assignment or amount of participation of the Principal Investigator designated on the title page.

d. Assure that the research is completed and the final report is delivered to RDL not later than twelve months from the effective date of this subcontract, but no later than December 31, 1998. The effective date of the subcontract is one week after the date that the institution's contracting representative signs this subcontract, but no later than January 15, 1998.

e. Assure that the final report is submitted in accordance with Attachment 3.

f. Agree that any release of information relating to this subcontract (news releases, articles, manuscripts, brochures, advertisements, still and motion pictures, speeches, trade associations meetings, symposia, etc.) will include a statement that the project or effort depicted was or is sponsored by: Air Force Office of Scientific Research, Bolling AFB, D.C.

g. Notify RDL of inventions or patents claimed as the result of this research as specified in Attachment 1.

h. RDL is required by the prime contract to flow down patent rights and technical data requirements to this subcontract. Attachment 2 to this subcontract

contains a list of contract clauses incorporated by reference in the prime contract.

4. All notices to RDL shall be addressed to:

RDL AFOSR Program Office
5800 Uplander Way
Culver City, CA 90230-6609

5. By their signatures below, the parties agree to provisions of this subcontract.

A S Sopher

Abe Sopher
RDL Contracts Manager

Signature of Institution Contracting Official

Typed/Printed Name

Date

Title

Institution

Date/Phone

ATTACHMENT 2
CONTRACT CLAUSES

This contract incorporates by reference the following clauses of the Federal Acquisition Regulations (FAR), with the same force and effect as if they were given in full text. Upon request, the Contracting Officer or RDL will make their full text available (FAR 52.252-2).

FAR CLAUSES	TITLE AND DATE
52.202-1	DEFINITIONS
52.203-3	GRATUITIES
52.203-5	COVENANT AGAINST CONTINGENT FEES
52.203-6	RESTRICTIONS ON SUBCONTRACTOR SALES TO THE GOVERNMENT
52.203-7	ANTI-KICKBACK PROCEDURES
52.203-8	CANCELLATION, RECISSION, AND RECOVERY OF FUNDS FOR ILLEGAL OR IMPROPER ACTIVITY
52.203-10	PRICE OR FEE ADJUSTMENT FOR ILLEGAL OR IMPROPER ACTIVITY
52.203-12	LIMITATION ON PAYMENTS TO INFLUENCE CERTAIN FEDERAL TRANSACTIONS
52.204-2	SECURITY REQUIREMENTS
52.209-6	PROTECTING THE GOVERNMENT'S INTEREST WHEN SUBCONTRACTING WITH CONTRACTORS DEBARRED, SUSPENDED, OR PROPOSED FOR DEBARMENT
52.212-8	DEFENSE PRIORITY AND ALLOCATION REQUIREMENTS
52.215-2	AUDIT AND RECORDS - NEGOTIATION
52.215-10	PRICE REDUCTION FOR DEFECTIVE COST OR PRICING DATA

52.215-12	SUBCONTRACTOR COST OR PRICING DATA
52.215-14	INTEGRITY OF UNIT PRICES
52.215-8	ORDER OF PRECEDENCE
52.215.18	REVERSION OR ADJUSTMENT OF PLANS FOR POSTRETIREMENT BENEFITS OTHER THAN PENSIONS
52.222-3	CONVICT LABOR
52.222-26	EQUAL OPPORTUNITY
52.222-35	AFFIRMATIVE ACTION FOR SPECIAL DISABLED AND VIETNAM ERA VETERANS
52.222-36	AFFIRMATIVE ACTION FOR HANDICAPPED WORKERS
52.222-37	EMPLOYMENT REPORTS ON SPECIAL DISABLED VETERAN AND VETERANS OF THE VIETNAM ERA
52.223-2	CLEAN AIR AND WATER
52.223-6	DRUG-FREE WORKPLACE
52.224-1	PRIVACY ACT NOTIFICATION
52.224-2	PRIVACY ACT
52.225-13	RESTRICTIONS ON CONTRACTING WITH SANCTIONED PERSONS
52.227-1	ALT. I - AUTHORIZATION AND CONSENT
52.227-2	NOTICE AND ASSISTANCE REGARDING PATIENT AND COPYRIGHT INFRINGEMENT

52.227-10	FILING OF PATENT APPLICATIONS - CLASSIFIED SUBJECT MATTER
52.227-11	PATENT RIGHTS - RETENTION BY THE CONTRACTOR (SHORT FORM)
52.228-7	INSURANCE - LIABILITY TO THIRD PERSONS
52.230-5	COST ACCOUNTING STANDARDS - EDUCATIONAL INSTRUCTIONS
52.232-23	ALT. I - ASSIGNMENT OF CLAIMS
52.233-1	DISPUTES
52.233-3	ALT. I - PROTEST AFTER AWARD
52.237-3	CONTINUITY OF SERVICES
52.246-25	LIMITATION OF LIABILITY - SERVICES
52.247-63	PREFERENCE FOR U.S. - FLAG AIR CARRIERS
52.249-5	TERMINATION FOR CONVENIENCE OF THE GOVERNMENT (EDUCATIONAL AND OTHER NONPROFIT INSTITUTIONS)
52.249-14	EXCUSABLE DELAYS
52.251-1	GOVERNMENT SUPPLY SOURCES

DOD FAR CLAUSES	DESCRIPTION
252.203-7001	SPECIAL PROHIBITION ON EMPLOYMENT
252.215-7000	PRICING ADJUSTMENTS
252.233-7004	DRUG FREE WORKPLACE (APPLIES TO SUBCONTRACTS WHERE THERE IS ACCESS TO CLASSIFIED INFORMATION)
252.225-7001	BUY AMERICAN ACT AND BALANCE OF PAYMENTS PROGRAM
252.225-7002	QUALIFYING COUNTRY SOURCES AS SUBCONTRACTS
252.227-7013	RIGHTS IN TECHNICAL DATA - NONCOMMERCIAL ITEMS
252.227-7030	TECHNICAL DATA - WITHOLDING PAYMENT
252.227-7037	VALIDATION OF RESTRICTIVE MARKINGS ON TECHNICAL DATA
252.231-7000	SUPPLEMENTAL COST PRINCIPLES
252.232-7006	REDUCTIONS OR SUSPENSION OF CONTRACT PAYMENTS UPON FINDING OF FRAUD

APPENDIX 2:

SAMPLE TECHNICAL EVALUATION FORM

SUMMER RESEARCH EXTENSION PROGRAMTECHNICAL EVALUATION

SREP NO: 95-0811
SREP PRINCIPAL INVESTIGATOR: Dr. Michael Burke

Circle the rating level number, 1 (low) through 5 (high), you feel best evaluate each statement and return thecompleted form by mail to:

RDL
Attn: 1995 SREP Tech Evals
5800 Uplander Way
Culver City, CA 90230-6608
(310) 216-5940 or (800) 677-1363

1.	This SREP report has a high level of technical merit.	1 2 3 4 5
2.	The SREP program is important to accomplishing the lab's mission.	1 2 3 4 5
3.	This SREP report accomplished what the associate's proposal promised.	1 2 3 4 5
4.	This SREP report addresses area(s) important to the USAF.	1 2 3 4 5
5.	The USAF should continue to pursue the research in this SREP report.	1 2 3 4 5
6.	The USAF should maintain research relationships with this SREP associate.	1 2 3 4 5
7.	The money spent on this SREP effort was well worth it.	1 2 3 4 5
8.	This SREP report is well organized and well written.	1 2 3 4 5
9.	I'll be eager to be a focal point for summer and SREP associates in the future.	1 2 3 4 5
10.	The one-year period for complete SREP research is about right.	1 2 3 4 5

---

11. If you could change any one thing about the SREP program, what would you change.

---

12. What would you definitely NOT change about the SREP program?

USE THE BACK FOR ANY ADDITIONAL COMMENTS.

Laboratory: Armstrong Laboratory
Lab Focal Point: Linda Sawin Office Symbol: AL/HRMI
Phone: (210) 536-3876

AEDC

PLANT-WIDE PREVENTATIVE MAINTENANCE AND MONITORING

Dr. Theodore A. Bapty
Dr. Janos Sztipanovits
Jason Scot
Brian Ball
Department of Electrical and Computer Engineering

Vanderbilt University
Nashville, TN 37235

Final Report for:
Summer Research Extension Program
Arnold Engineering Development Center

Sponsored by:
Air Force Office of Scientific Research
Bolling Air Force Base, Washington, D.C.

and

Vanderbilt University

December 1995

PLANT-WIDE PREVENTATIVE MAINTENANCE AND MONITORING

Dr. Theodore A. Bapty
Dr. Janos Sztipanovits
Jason Scott
Brian Ball

Measurement and Computing Systems Laboratory

Abstract

This research concentrated on developing methods for on-line analysis monitoring and analysis of large-scale plants. The target application, monitoring and diagnosis of a large motor control system, was chosen to focus the research on a specific need and to provide a arena for demonstrating the technology through a prototype system. The criticality of the motor system to AEDC, the cost of an undetected fault, and the difficulty of diagnosis guided the selection of this particular application.

In the course of the work, several new algorithms were developed for diagnosis of the power control circuits. The algorithms take advantage of Ordered Binary Decision Diagrams (OBDD) to manage the complexity of system diagnosis. These algorithms were incorporated into an on-line monitoring system for connection directly to the motor circuit. The approach uses the circuit diagrams as Models. These models are interpreted to generate the diagnostic/monitoring system.

PLANT-WIDE PREVENTATIVE MAINTENANCE AND MONITORING

Dr. Theodore A. Bapty
Dr. Janos Sztipanovits
Jason Scott
Brian Ball

INTRODUCTION

This research concentrated on developing methods for on-line analysis monitoring and analysis of large-scale plants. The target application, monitoring and diagnosis of a large motor control system, was chosen to focus the research on a specific need and to provide a arena for demonstrating the technology through a prototype system. The criticality of the motor system to AEDC, the cost of an undetected fault, and the difficulty of diagnosis guided the selection of this particular application.

The need for this research became apparent through participation in the Summer Research Program (SRP) at Arnold Engineering Development Center (AEDC). This report documents the results of a follow-up grant (mini-grant) awarded as an extension of the SRP.

In the course of the work, several new algorithms were developed for diagnosis of the power control circuits. The algorithms take advantage of Ordered Binary Decision Diagrams (OBDD) to manage the complexity of system diagnosis. These algorithms were incorporated into an on-line monitoring system for connection directly to the motor circuit. The approach uses the circuit diagrams as Models. These models are interpreted to generate the diagnostic/monitoring system.

MOTIVATION

Arnold Engineering Development Center operates the largest, most diverse complex of aerospace testing facilities in the world. These facilities range from turbine engine test cells, to wind tunnels, to space chambers, to hyperballistic test ranges, to rocket test cells. Accurate simulation of conditions is a key attribute of AEDC testing. For turbine engine testing, this means that air is conditioned to temperatures, pressures, and mass flow rates encountered by a full-scale engine operating as part of an aircraft. For wind tunnels, the air must be conditioned to conditions to allow a scaled-down model to achieve full scale behavior.

In order to provide these simulated conditions, a very large complex of machinery is required. For turbine engine testing, the Aerospace System Test Facility(ASTF) uses 6 large 60,000 horsepower motors to compress air through heaters and coolers to provide the input airstream to the test article. Another set of 12 motors extracts the air from the turbine engine

under test to simulate altitude operation. A complex network of valves and pipes routes the air throughout the facility to provide a dynamic simulation of engine environments.

Within AEDC, there are 6 major turbine engine test facilities, with multiple air supply and exhaust systems. The motors used in these facilities range in age from 10 to 50 years. Many of them are irreplaceable. The costs to repair and rewind one of these motors is on the order of $3 Million. More significantly, the downtime of the facility is very expensive, due to the $20K per hour value of testing time. The impact of testing delays can propagate to expenses in the aircraft system development projects.

One can see the importance of the correct functioning of the large motors to the operations at AEDC. For this reason, the motor control system was chosen as a target domain.

The primary objective of this effort is to develop tools for the diagnosis of the large electric motor systems. Since the motor itself is a relatively simple mechanism, the diagnosis efforts focused on the control system and the environmental factors, i.e. power supply. These factors cover the majority of the operating failures in the AEDC large motor complex. For problems within the motor, indications are available at the power supply. The causes and indications of failure of the motor systems addressed this work included only the electrical systems. The factors due to mechanical problems (bearings, shaft imbalance, system resonances) were not considered within this project, due to the small scope. This is not to say that these factors are not important: bearing wear can cause substantial problems. This information should be considered as a follow-on effort.

The efforts will be described in the following sections. We begin with the control system diagnosis efforts, followed by the power analysis results.

CONTROL SYSTEM DIAGNOSTICS

These systems consist of a complex set of interlocks to cycle the motor through its startup phase, and to monitor for shutdown conditions. The control system determines when the motor is supplied with power and when the power should be removed. Errors in the control system result in improper motor functioning. In the best case, the motor function is somewhat impaired or the motor stops. A more serious malfunction could damage the motor. For these reasons, the correct functionality of the control system is critical.

The control system is implemented in standard relay ladder logic. In order to manage the complexity of this subsystem, we have chosen to use models to represent its behavior. Models have been used throughout history as a way of managing complexity. The Measurement and Computing Systems Laboratory at Vanderbilt has been conducting research for the past 8 years on using models to describe complex systems. The Model-Based approach, which we call the Multigraph System Architecture, has proven to be effective in several diverse diagnostics and

monitoring domains (see, for example, [1], [2], [3]).

The essence of this approach is as follows:

- Define a Modeling Paradigm. The paradigm defines the key concepts necessary to capture information necessary to describe the system to be monitored and diagnosed. The paradigm uses concepts familiar to the domain, allowing the system to be expressed in a straightforward, natural manner. Proper choice of paradigm concepts is critical for completeness of representation and for ease of interpretation.
- Implement a modeling editor. The editor is a graphical Computer Aided Design (CAD) tool that implements the modeling paradigm. The model editor allows the designer to easily describe and input models of the system.
- Implement an Interpreter for the models. The interpreter processes the models defined in the modeling editor and produces executable systems. This process is tailored to both the modeling paradigm and the target execution system. The interpreter performs a mapping from the model paradigm to the execution system.
- Implement an Execution Support System. This software layer allows direct execution of the output of the model interpreter. The form of the execution layer is dependent upon the application domain. The Multigraph Kernel provides a Large-Grain Dataflow environment for implementation of parallel processing applications. Diagnosis applications build a layer atop the kernel, to directly support diagnosis applications. The relay ladder logic of the physical motor control system implements an finite state machine. This system is implemented in terms of relays (Coils and Contacts), externally driven contact closures and disconnects, fuses and circuit breakers, and a network of wires connecting these components.

Since the goal of this project is to diagnose failures in the control system, we must consider the types of failures that occur within the system. These are:

- **Relay Contact Closure Stuck Open**. Due to a mechanical failure of a specific contact or a failure of the control coil.
- **Relay Contact Closure Stuck Closed**. Due to a mechanical failure of a specific contact or a failure of the control coil.

The most natural method of modeling these systems is to mimic the standard way of representing the designs: A schematic. Within the modeling environment the following concepts will be implemented:

- **COMPONENTS** drawn within a schematic. The supported components are:
  - Externally-Driven Relay Contact: Normally Open.
  - Externally-Driven Relay Contact: Normally Closed.
  - Coil-Driven Relay Contact: Normally Open.
  - Coil-Driven Relay Contact: Normally Closed.

- Circuit Breaker.
- Resistor.
- Wire.

All of these components, with the exception of the Wire, have two connection points. Wires have only one logical connection point, as the electrical potential is equivalent throughout a set of connected wires.

- **CONNECTIONS** The components can be connected, forming an electrical connection. Connections of wires form an electrical network. The allowable connections are:

  - Wire-to-Wire, forming a net.
  - Wire-to-Component, connecting a component to a network.

- **COIL-CONTACT RELATIONS** These relationships define the interaction between energizing a coil and closure or opening of a contact.

These model concepts and components are used to draw the control circuit within the Model-Builder. The information necessary to build the models is available in standard schematic diagrams. These models will be interpreted to construct system descriptions suitable for the diagnostics algorithms. These algorithms will be described in the next section.

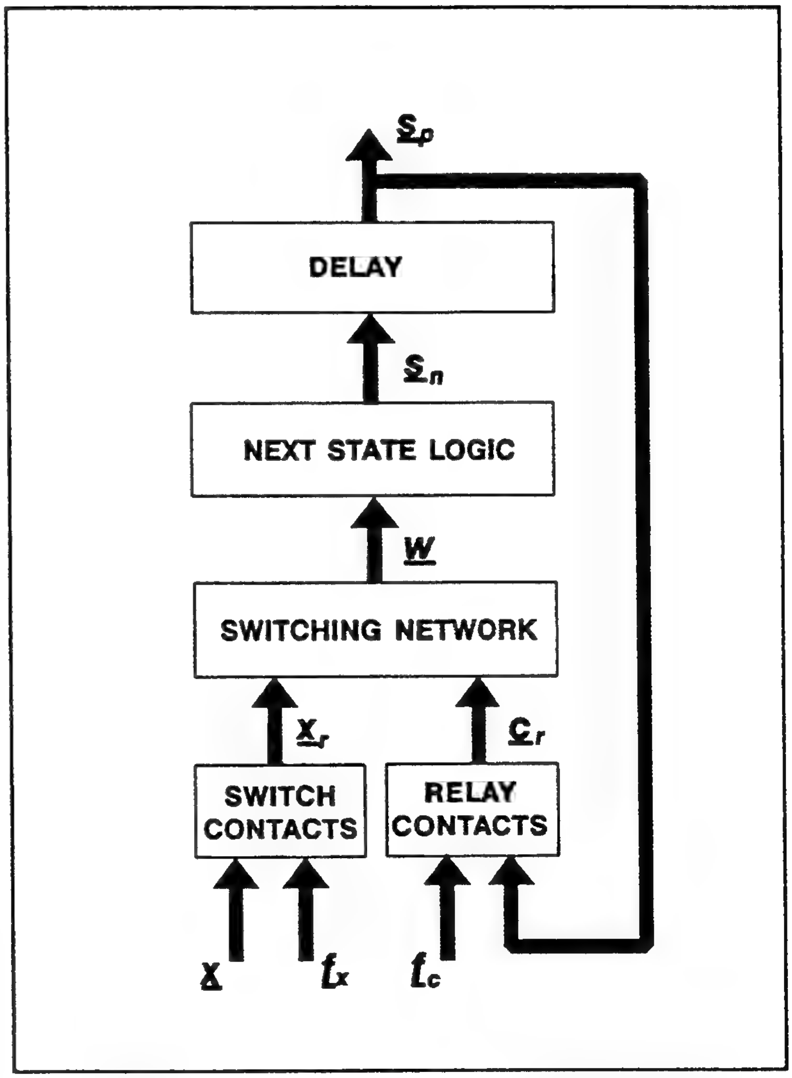

Figure 1: AFSM Model of the control circuit

DIAGNOSTICS ALGORITHMS

The goal of the diagnostic system is to find the faulty components using observations. Since the structure and expected ideal behavior of the control circuit is known, we choose a

model-based diagnostic system approach for solving the task. In model-based diagnostics a model of the system is used to generate possible faulty behaviors. In this process fault hypotheses are introduced in the model, and the model-generated faulty behavior is compared with actual measurements. If the measured and model-generated behaviors are the same, the related fault hypotheses are accepted as possible explanations for the fault symptoms. Typically, there are many fault hypotheses that can explain a particular fault symptom. In these cases, the diagnostic system selects the simplest possible explanation, i.e. the one, which includes the least number of independent fault assumptions.

1. System model

The model-based diagnostic system requires a system model, which is able to explain the possible behaviors in terms of component characteristics. The control circuit is a relay logic, comprising switches, relays and contact points. This system is modelled as an asynchronous finite state machine (ASFM), as shown in Figure 1. The components of the ASFM model are the following:

State variables: The relays have two possible states, 'energized' and 'not-energized', therefore their states are modelled with Boolean variables. Due to the loops in the switching network, the relay states are considered to be the state variables of the controller represented by the Boolean state vector $\underline{s}$. The state vector has a 'present state', $\underline{s}_p$, and a 'next state' $\underline{s}_n$ value connected by an asynchronous delay block. The asynchronity of the state machine means that only one of the state variables changes in the same time.

Next State Logic: The relays are energized by the potential difference appearing on the 'wires' which are connected to the terminals of the relay coils. The 'Next State Logic' is represented by the Boolean expressions describing the next state, $\underline{s}_n$ of the state variables in terms of the states of the 'wires'. The state of the wires is characterized by the Boolean vector $\underline{w}$. The state of the wires (the wire is 'energized' or 'not-energized') are the directly 'observable' variables in the system.

Switching Network: The state of the wires is determined by the state of the relay contacts, the state of the switches and the topology of the switching circuit. The state of the switches and relay contacts can be 'open' or 'close'. These states are modelled by the Boolean vectors $\underline{c}_r$ and $\underline{x}_r$.

Switch Contacts: The switch contacts are one of the fault sources in the control circuit. The fault model of the contact points is 'stuck open' and 'stuck close'. The Switch Contact network models the 'real' switch contact points as a logic

function of the ideal switch contact state $\underline{x}$ and a fault vector $\underline{f}_x$. The logic expression for the fault model of the *ith* contact point is the following:

$$x_r(i) = x(i) \wedge \neg x\_fo(i) \vee x\_fc(i),$$
$$x\_fo(i) \wedge x\_fc(i) = 0$$

where $x_r(i)$ is the *ith* real contact point, $x(i)$ is the corresponding ideal contact point, $x\_fo(i)$ is the 'stuck open' failure and $x\_fc(i)$ is the 'stuck close' failure.

Relay Contacts: The relay contacts represent the contacts points controlled by the state of the relays. A relay contact can be 'normally closed' or 'normally open'. The logic relationship between the $s(k)$ state variable and the related, $c\_sk(i)$ 'normally closed' and $c\_sk(j)$ 'normally open' contact points is:

$$c\_sk(j) = s(k) \quad \text{(normally open)}$$
$$c\_sk(i) = \neg s(k) \quad \text{(normally closed)}$$

The fault model of the relay contact points is the same as that of the switch contact points.

Given an initial state $\underline{s}_0$ and an input switch setting $\underline{x}_i$, the state machine will go through a state trajectory and stabilizes in a new state $\underline{s}(\underline{s}_0,\underline{x}_i)$. If the switch and relay contacts are not faulty, the stabilized new state will be the required state, which e.g. starts up an electric motor. If contact points are faulty, a the resulting new state may be incorrect, even not stable.

The goal of the diagnostic reasoning is to identify possible fault causes based on the full, or partial observation of the state trajectory.

2. Relational model

The main problem with the diagnostics of AFSM systems described above is the very large space of possible behaviors of the system. Any attempt to perform diagnostic reasoning using pattern matching seems to be hopeless, since in systems of realistic size the fault patterns can not even be enumerated, let alone used in pattern matching.

A promising approach to solve the state explosion problem is to use symbolic reasoning. In the symbolic approach, representations focus not on the individual instances of variables, but on sets and relations representing possible states, fault hypotheses, constraints, etc. Sets and relations can be efficiently represented symbolically using Ordered Binary Decision Diagrams (OBDD) [1].

The relational model of the AFSM describes the system in terms of sets and relations as shown in Figure 2. The sets represent all possible states of functional components of the AFSM. The sets are constrained by relations which are derived from the circuit specification. For example, the set W includes all of those $w \in W$ states of the wires that can be energized in the same time given the operational constraints of control circuit. The state w is coded by the Boolean vector $\underline{w}$, i.e. by the states of the individual wires.

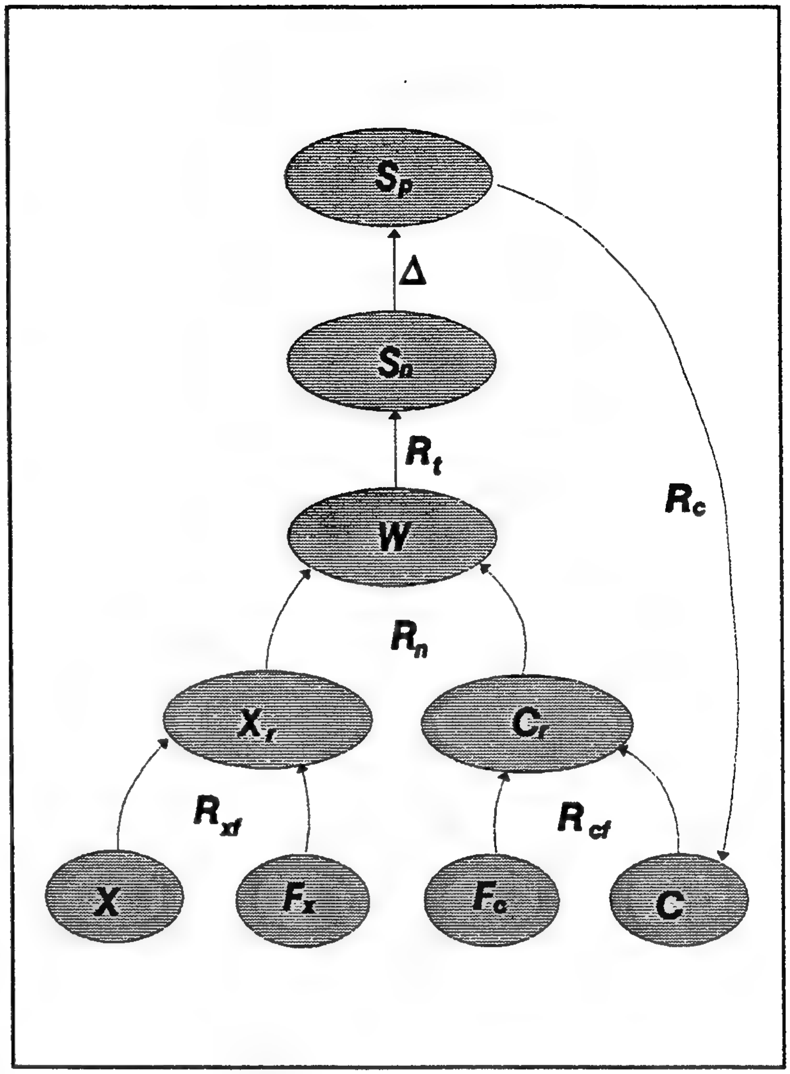

Figure 2: Relational model of the control circuit

The relations of the AFSM are the following:

a) Delay

$$\Delta = s_n(i) \Leftrightarrow s_p(i) \ \ \forall\, i$$

b) State transition relation

$$R_t = R_t(0) \lor R_t(1) \lor \ldots \lor R_t(n\text{-}1)$$

$$R_t(i) = \ s_n(i) \Leftrightarrow T_i(\underline{w}) \land (s_n(i) \oplus s_p(i)) \land \bigwedge_{j \neq i} (s_n(j) \Leftrightarrow s_p(j))$$

where $T_i(\underline{w})$ is a Boolean expression describing the next state of the state variable $s_n(i)$ as the function of the state of the wires, and n is the number of state variables (i.e. relays).

c) Network relation

$$R_n = R_n(0) \wedge R_n(1) \wedge \ldots \wedge R_n(m-1)$$

$$R_n(i) = w(i) \Leftrightarrow N_i(\underline{x}_r, \underline{c}_r)$$

where $N_i(\underline{x}_r, \underline{c}_r)$ is a Boolean expression describing the state of the wire $w(i)$ in terms of the state of the 'real' switching contacts $\underline{x}_r$ and the state of the 'real' relay contacts $\underline{c}_r$, and m is the number of wires in the network.

d) Switching contact relations

$$R_{xf} = R_{xf}(0) \wedge R_{xf}(1) \wedge \ldots \wedge R_{xf}(p-1)$$

$$R_{xf}(i) = x_r(i) \Leftrightarrow (x(i) \wedge \neg x\_fo(i) \vee x\_fc(i)) \wedge (\neg x\_fo(i) \vee \neg x\_fc(i))$$

where p is the number of switching contact points.

e) Relay contact relations

$$R_{cf} = R_{cf}(0) \wedge R_{cf}(1) \wedge \ldots \wedge R_{cf}(n-1)$$

$$R_{cf}(i) = R_{cf}(i,0) \wedge R_{cf}(i,1) \wedge \ldots \wedge R_{cf}(i,q_i-1)$$

$$R_{cf}(i,j) = c_r(i,j) \Leftrightarrow (c(i,j) \wedge \neg c\_fo(i,j) \vee c\_fc(i,j)) \wedge (\neg c\_fo(i,j) \vee \neg c\_fc(i,j))$$

where $c_r(i,j)$ is the Boolean variable representing the *jth* 'real' contact point of the *ith* relay, and q_i is the number of contact points belonging to relay i.

f) Relay constraints

$$R_c = R_c(0) \wedge R_c(1) \wedge \ldots \wedge R_c(n-1)$$

$$R_c(i) = R_c(i,0) \wedge R_c(i,1) \wedge \ldots \wedge R_c(i,q_i-1)$$

$$R_c(i,j) = c(i,j) \Leftrightarrow s_p(i)$$

where $c(i,j)$ is the Boolean variable representing *jth* (normally open) 'ideal' contact point of the *ith* relay.

3. Prediction and diagnostics

Having the relational model defined, the model can be used for prediction and diagnostics.

In prediction, assuming a set of initial states $s_p \in S_p$, an input switch position setting x, and a given fault scenario f_c and f_x, the set of next states $s_n \in S_n$ is calculated. The 1-step prediction function is defined as follows:

$$P(S_p,x,f_c,f_x) = \{s_n \mid \exists\, s_p,c,c_r,w[(s_p \in S_p) \wedge ((s_p,c) \in R_c) \wedge ((f_c,c,c_r) \in R_{cf}) \wedge ((x,f_x,x_r) \in R_{xf}) \wedge \wedge ((x_r,c_r,w) \in R_w) \wedge (w,s_n) \in R_t\,]\}$$

Given the 1-step predictor function, reachability and stability analysis can be performed.

In diagnostics, the sets in the relational model are propagated backward. It is important to note that the relational model is not changing, only the propagation mechanism. This time we describe the only the batch diagnostic method. In batch diagnostics, the operation of the control system is observed, and the results are collected in the [$\underline{m}(1)$, $\underline{m}(2)$, ... $\underline{m}(i)$] measurement vector sequence. The components of the $\underline{m}(i)$ vector are the states of the observed wires at time i. The diagnostics function is defined as a recursive function, which propagates backward the states and fault hypotheses along the fully or partially measured values of the system trajectory. The 1-step backward propagation function calculates the previous state set, $s_p \in S_p$, the previous wire state set $w_p \in W_p$, and the previous fault hypotheses sets, $f_{cp} \in F_{cp}$ and $f_{xp} \in F_{xp}$, given the current state set, $s_n \in S_n$, current fault hypotheses sets, $f_{cn} \in F_{cn}$ and $f_{xn} \in F_{xn}$, current wire state set $w_n \in W_n$, and measurement vector $m(i)$:

$$B(S_n,F_{cn},F_{xn},W_n,x,m(i)) = \{s_p, f_{cp}, f_{xp}, w_p \mid \exists\, s_n,c,c_r,f_{cn}, f_{xn}, w_n[(s_n \in S_n) \wedge (f_{cn} \in F_{cn}) \wedge (f_{xn} \in F_{xn}) \wedge \wedge (w_n \in W_n) \wedge (f_{cp} \in F_{cn}) \wedge (f_{xp} \in F_{xn}) \wedge ((s_p,c) \in R_c) \wedge ((f_{cn},c,c_r) \in \in R_{cf}) \wedge ((x,f_{xn},x_r) \in R_{xf}) \wedge ((x_r,c_r,w) \in R_w) \wedge ((w,s_n) \in R_t\,)(m(i) \in \in W_n)]\}$$

Both the forward and backward propagation functions can be calculated symbolically using the OBDD representation of the sets and relations. The repeated application of the forward propagation function generates the reachability set, the repeated application of the backward propagation function results in a fault hypothesis set.

DIAGNOSTICS EXECUTION ENVIRONMENT

By interpreting the models, we can generate specifications for an on-line runtime system. This system allows the user to:

- Acquire data from the physical control system. Data is logged and time-tagged whenever the state of a sensor changes. An arbitrary number of sensors is supported. The current number is 24 or 48. Sample rate is adjustable. The hardware implementation of the data acquisition system will be discussed later.

- Visualize the current state of the network. To facilitate the visualization, a circuit schematic diagram is drawn on the screen. The voltage state of each wire is represented by the color of the wire: Red for high, black for low. The component states are shown by changes in the icons. Activated coils change color and closed contacts change visual appearance.

The user interface allows the user to zoom in on areas of the schematic and to scroll around.

- Step through the historical data to visualize system events at a user-controlled pace. This allows the user to recreate events in a time-scale visible to a human.
- Execute the diagnostics starting from any place in the acquired data log. The diagnostics can be executed in a forward simulation mode or in a reverse-time mode.
- Visualize the results of the diagnostics. Suspect components are highlighted in the schematic display along with a verbal description. The user interface was implemented in Microsoft Visual C++. The system executes under Windows 95, for maximum flexibility and ease of training (most users already know how to use windows applications).

POWER SYSTEMS ANALYSIS

A parallel effort focused on the conditions of the power supply feeding the motor. This phase attempts to find current and impending problems by monitoring the current and voltage of the main power feed to the motor.

For a standard, problem free motor startup the design parameters of the system specify a range of current and voltages. The first-level monitoring system watches the data online for deviations outside the design ranges. Excursions are flagged and noted to a history log.
Each motor startup profile is logged and parameterized. The parameters for startup characterization include rise-time, slope, and damping parameters for the startup transient. These parameters can be plotted versus time to detect degradations in the motors.

The power consumption curve also corresponds to mechanical motor load. By watching instantaneous Voltage*Current load fluctuations can be observed. Changing load profiles can also indicate changes in motor behavior.

The current user interface does not include the power system analysis. Live data from motor start-up was not available. Consequently, the algorithms were not able to be validated within the time frame of this project.

DATA ACQUISITION SYSTEM

The data acquisition system used off-the-shelf hardware where possible along with

custom-designed interface circuitry.

The motor control circuits operate on 125 VDC. These voltages are too high to feed directly into standard computer input devices, which operate on 5 VDC. Direct contact of 125V at the computer interface will damage the circuitry. To convert between these voltage levels and to isolate and protect the computer, a circuit was developed.

The circuit consists of an optoisolator and a buffer. The 125 VDC is connected to the input to the optoisolator through a current-limiting resistor. The output of the optoisolator drives a TTL schmitt trigger buffer to reduce noise from switch bounce and further protects the computer.

The computer interface was implemented using QUA-TECH digital I/O boards, since they were available in the lab. Each of these boards can acquire 24 digital inputs. Any number of these boards can be used in a single computer, limited only by expansion slots.

CONCLUSIONS/RECOMMENDATIONS

Due to the late decision on the target application, and to delays in acquiring information from the Air Force contact, the development of the integrated diagnostics system has not yet been completed. The work on integration of the prototype will continue to bring the prototype to completion. This prototype will be installed at AEDC to evaluate the effectiveness of the approach. We expect to demonstrate the prototype in late January, 1996. The results of the prototype evaluation will be described in an appendix to this report.

The diagnostics methods developed for the relay logic control circuit have been proven effective in managing complexity. The original approach was to describe all possible faults and system failures possible in the operation of the system. Enumerating all of the failure modes is a tedious, labor intensive, error prone process. The resulting fault tree would be very large, with no method for assuring complete system coverage. The OBDD approach for the execution system support automatically ensures complete fault coverage. This approach also serves to reduce diagnosis algorithm complexity, contributing to system scalability. On the sample application, the system executes efficiently. The scalability has been indicated by gradually increasing the fidelity of the diagnosis, with moderate increases system execution times.

The work with the motor startup curve analysis has been entirely theoretical, due to the lack of real data. For health monitoring, this data can be invaluable in detecting changes in system operation. Analysis results look promising. Availability of high speed signal processing hardware (see [1]) demonstrates the feasibility of performing this analysis full-time at very low cost. We recommend that these approaches be further developed. The electrical aspect of the motors is just one part of the operation of a large system. Problems in the mechanical implementation of the system can also cause problems, such as bearing wear, shaft imbalance, and gearbox resonances. To detect and analyze these types of problems, the mechanical system

must be instrumented with accelerometers, vibration sensors, and possibly audio sensors. Analysis of these signals can help detect these problems and determine the root causes of the fault. Since a failure in any aspect of the system becomes apparent in all aspects of the system, indications are visible in all methods of monitoring the system. The most accurate system diagnosis will consider all of these failure indicators. We recommend integrating all aspects into a single system.

ACKNOWLEDGEMENTS

We wish to thank the Air Force Material Command and the Air Force Office of Scientific Research for sponsorship of this research. Research Development Labs must also be commended for their concern and help to us in all administrative and directional aspects of this program.

Tom Tibbals was extremely helpful in overcoming many technical roadblocks in the selection of the target application. Mike Shuran offered enthusiastic support in describing the application domain acquiring the information necessary to model the system. He will be invaluable in integrating the prototype into use at AEDC.

REFERENCES

[1] Bapty, T., et al.: "Parellel Turbine Engine Instrumentation System," Proc. of the (5th AIAA Conference on Computing in Aerospace, San Diego, CA, Oct. 1993

[2] Karsai, G.: "A Configurable Visual Programming Environment: A Tool for Domain-Specific Programming," Computer, March 1995

[3] Misra, A., et al.: "Diagnosability Analysis and Robust Diagnostics with Multiple Aspect Modeling," Abstracts of the NASA Workshop on Model-Based Diagnosis and Monitoring, Pasadena, CA, Jan. 1992

FJSRL

BLOCK COPOLYMERS AT INORGANIC SOLID SURFACES

John R. Dorgan

Assistant Professor

Department of Chemical Engineering and Petroleum Refining

Colorado School of Mines

1500 Illinois Street

Golden, Co 80401-1887

Final Report for:

AFOSR Summer Research Extension Program

Research & Development Laboratories

5800 Uplander Way

Culver City, CA 90230-6608

Sponsored by:

Air Force Office of Scientific Research

and

Frank J.Seiler Research Laboratory

May 1996

BLOCK COPOLYMERS AT INORGANIC SOLID SURFACES

John R. Dorgan
Assistant Professor
Department of Chemical Engineering and Petroleum Refining
Colorado School of Mines

Abstract

Polymer molecules attached to a solid surface are of extreme technological interest. Thin polymer films find widespread use in many industries and improvements in thin films will lead to superior technologies.

In this study, we report the first experimental results on the scaling characteristics of brush-forming middle-adsorbing triblocks. The triblocks used consist of relatively short poly(ethylene oxide) (PEO) middle blocks and much longer polystyrene (PS) end blocks. Adsorption takes place onto a well characterized silicon dioxide surface from toluene and ellipsometry is used to determine the adsorbed amount. We find that the surface density, σ, for all of the copolymers (both those in the symmetric and asymmetric regimes) scale according to the simple relationships proposed in the theory of Marques and Joanny i.e. in the symmetric to moderately symmetric regime, $\sigma \approx \frac{1}{N_A}$, where N_A is the number of segments in the adsorbing PEO block and in the highly asymmetric regime, $\sigma \approx \frac{1}{\beta^2}$, where β is the ratio of the size of the non-adsorbing block to the size of the adsorbing block.

BLOCK COPOLYMERS AT INORGANIC SOLID SURFACES

John R. Dorgan

Introduction

Polymer coils terminally attached to a solid surface constitute an interface of particular interest. For example, they are used in the stabilization and flocculation of colloidal particles such as those used as precursors to the sintering of ceramics[1] Uses in biomedical technology include affinity chromatography and the enhancement of biocompatibility of artificial implants. These materials should also prove useful for electrode modification. Composite materials consisting of adsorbed polymer chains can be said to represent the ultimate in polymer thin films; a single layer of polymer coils attached to a solid surface. Such thin polymer films are desirable for many applications in electronics and optoelectronics where film properties must be closely controlled.

Objective

The objective of the project was to establish structure-property relationships for polymer films formed via the adsorption of block copolymers and to test relevant theories of copolymer adsorption. The specific case of copolymers to be studied was the middle-adsorbing triblock copolymers.

Background

For an isolated polymer coil in solution, the natural size of the molecule to consider is the Flory radius, R_F. In a good solvent, the Flory radius scales with the number of repeat units raised to the three-fifths power; this scaling behavior represents a trade-off between the entropic penalty of stretching the coil and its preference to avoid self-interaction and promote polymer-solvent contacts[2] If a polymer molecule is attached to a solid surface in the presence of other polymer molecules, then the interchain spacing can become less than the Flory radius. In such a situation the chains stretch away from the surface and into the solvent - such a structure is known as a polymer brush[3] This stretching feature of polymeric materials makes them unique and contrasts them with low molecular weight materials which face different packing constraints at interfaces.[4]

With copolymers, it is possible to have segments in the polymer chain which adsorb and segments which do not. In the discussion which follows the usual notation is adopted and the β parameter is defined as the ratio of the size of the nonadsorbing (Buoy) block to the size of the adsorbing (Anchor) block

$$\beta = \frac{R_{F,B}}{R_{F,A}} = \frac{a_B N_B^{0.6}}{a_A N_A^{0.6}} = a'(N_B/N_A)^{0.6} \tag{1}$$

In Equation 1, a_A and a_B represent the monomer sizes within the anchor and buoy blocks, respectively, while N_A and N_B represent the number of monomers in each of these blocks. The grafting density of polymer chains at the surface also proves to be an important variable in the description of polymer brushes. The grafting density σ is simply related to the interchain spacing D through $\sigma = (1/D)^2$ and represents the number of chains per unit area. A schematic representation of a polymer brush in which these various definitions are illustrated is shown in Figure 1.

Scaling Theory

For the current work, the scaling theories of interest are those involving the adsorption from non-selective solvents. Marques and Joanny proposed three different regimes of symmetry for the case of diblocks. The results of their scaling treatment are shown in Table 1.[5] However, as pointed out by Guzonas et al, the predicted scaling behavior in two of the three regimes is similar and hence they suggested a slightly different classification based on the value of β; Copolymers with $\beta > N_A^{0.5}$ are identified as highly asymmetric (Tail regime), those with $1 < \beta < N_A^{0.5}$ as moderately asymmetric and those with $\beta < 1$ as symmetric (Head regime).[6] The crossover at $N_A^{0.5}$ is indicative of crossover from the head regime (in which the size of the adsorbing block dictates the surface coverage) to the tail regime (in which the excluded volume interactions of the nonadsorbing blocks dictates the surface coverage).

β	$1<\beta<N_A^{0.5}$ 3D regime	$N_A^{0.5}<\beta<N_A^{0.75}$ 2D semidilute	$\beta>N_A^{0.75}$ 2D dilute
$\sigma\sim$	N_A^{-1}	β^{-2}	β^{-2}
$L\sim$	$N_B N_A^{1/3}$	$N_B^{3/5} N_A^{2/5}$	$N_B^{3/5} N_A^{2/5}$

Table 1 : Scaling treatment of Marques and Joanny for the surface density and the thickness of the brush layer for diblocks.

Hence, the relative sizes of the two blocks play an important role in determining the structure of the surface layer. There are two possible structues : either a thick, "fluffy", continuous adsorbed layer or a thin layer which may be continuous or discontinuous.

Methods

The primary experimental tools used in this investigation were Low Angle Laser Light Scattering (LALLS), ellipsometry (ELLI) and Gel Permeation Chromatography (GPC). Ellipsometry is one of the few techniques which has the capability to simultaneously measure film thickness and grafting density. In order to appreciate this point, ellipsometry is now briefly reviewed; a more complete description of the technique is readily available in the literature. [7]

With a linear polarizer and a half wave plate it is possible to generate a known state of elliptical polarization, when reflected from a substrate the polarization of the light is changed. The intensity of light passing through the analyzer (a second motorized rotating linear polarizer) is monitored using a photodiode. From a Fourier analysis of the intensity signal, the two ellipsometric angles Δ and Ψ, are found. The fundamental relation of ellipsometry relates refractive indices (n_k) and layer thicknesses (d_k) of the reflecting surface to the measured angles Δ and Ψ.

$$e^{i\Delta} \tan\Psi = \frac{R_p}{R_s} = F(n_k, d_k) \qquad (2)$$

where n_k and d_k refer to the indices of refraction and thicknesses of each layer present (denoted by the subscript k). Measurement of the two independent quantities, Ψ and Δ usually allows for the solution of two unknowns, a layer

thickness, d_1 and a refractive index, n_1. A separate determination of n_1 and d_1 can be difficult and sometimes impossible due to the small differences in indices of refraction of the adsorbate and solution. A set of ellipsometric angles, Ψ and Δ can be produced by a higher refractive index, n_1 and a lower thickness, d_1 as also a lower refractive index, n_1 and a higher thickness, d_1; but the product $n_1 d_1$ is an invariant of the adopted layer model.[8]

For the study of adsorption, such a layer thickness and index of refraction can be found by assuming a homogeneous layer. The adsorbed amount may then be calculated as:

$$A = d_l c_l = d_l (n_l - n_o) / (dn/dc)_o \tag{3}$$

Where n_1 represents the index of refraction of the adsorbed layer, c_l is the concentration in the layer and d_1 the thickness, n_0 represents the index of refraction of the polymer solution and $(dn/dc)_0$ is the change in refractive index of the solution with concentration of the adsorbing species. It has been shown that the adsorbed amount, A, proves insensitive towards which type of concentration profile exists near the surface.

Knowing the adsorbed amount, the grafting density, σ, is calculated from Equation 4.

$$\sigma\,(\text{chains}/\text{nm}^2) = \frac{A(\text{mg}/\text{m}^2)}{M_w(\text{mg}/\text{mol})} N_{av}(\text{chains}/\text{mol}) \times 10^{-18} (\text{m}^2/\text{nm}^2) \tag{4}$$

The interchain spacing may then be calculated as:

$$D = (1/\sigma)^{0.5} \tag{5}$$

Further, the chain spacing at which coils on the surface first begin to touch is taken as:

$$D_{OVER} = (\pi R_B^{\,2})^{0.5} \approx (\pi R_{AB}^{\,2})^{0.5} \tag{6}$$

where R_B represents the radius of gyration of the polystyrene blocks in solution and R_{AB} is the radius of the copolymer in solution, determined by using light scattering.

The ellipsometer was modified to enable in-situ studies of the adsorption studies. The details of the modification to accomodate the solution cell can be found in previous works by Dorgan et al.[9]

Low angle laser light scattering (LALLS, Wyatt Technologies DAWN B) was used to measure weight-average molecular weights and the radii of gyration of the copolymer in solution. The polydispersity was determined using gel permeation chromatography (GPC).

Experiments

In this study, we report on the adsorption behavior of middle-attaching triblocks. The materials employed consist of relatively short poly(ethylene oxide) (PEO) blocks capped by relatively long polystyrene (PS) blocks. The PEO block preferentially adsorbs to the surface whereas the PS block remains dangling in solution. Adsorption takes place from toluene, a good solvent, onto a well characterized silicon oxide surface; this is a case of adsorption from a non-selective solvent onto a selective surface.

The copolymers used in this study have the characteristics shown in Table 2. The triblocks were synthesized at the Technical University of Istanbul by a procedure described earlier.[10] It is seen that the composition of the samples are such that the different regions of symmetry are covered (i.e.copolymers with $\beta < N_A^{0.5}$ lie in the symmetric to moderately symmetric regime and polymers with $\beta > N_A^{0.5}$ lie in the highly asymmetric regime). The silicon wafers are obtained from Silicon Source Inc. (Phoenix) and treated as described in previous works.[11] The film thickness of the oxide layer is independently determined prior to the adsorption run using ellipsometry. HPLC grade toluene (Aldrich Chemicals) was used after filtering three times through 0.2 micron Whatman filters. The adsorption experiments are all conducted at solution concentrations of 1.00 ± 0.01 mg/ml. Low angle laser light scattering (Wyatt Technologies DAWN B) was used to measure weight-average molecular weights and the radii of gyration of the copolymer in solution; no evidence of micelle formation is present at the concentrations used in the experiments. Figure 2 shows a Zimm plot for the sample PS(107k)-PEO(20k)-PS(107k). The polydispersity was determined using gel permeation chromatography (GPC) and seen to be less than 3.0 for all samples ($M_w / M_N < 3.0$). A specially modified rotating analyzer ellipsometer (Gaertner Scientific) is used to measure the adsorbed amounts.

The data analysis is performed as described in previous section.

Results and Discussions

Results from the study are given in Table 2. It is clearly seen that the ratio of the interchain spacings to the overlap spacings (D / D_{OVER}) are less than unity demonstrating that the triblock materials must be stretched

away from the adsorbing surface. To our knowledge, this is the first report of brush formation in copolymers of the B-A-B architecture.

Material	β	$N_A^{0.5}$	D (Å)	D / D_{OVER}
PS(254k)-PEO(54k)-PS(254k)	1.97	35.03	284.80	0.5551
PS(59k)-PEO(1k)-PS(59k)	9.16	4.7	138.50	0.3176
PS(22k)-PEO(1k)-PS(22k)	5.07	4.7	68.33	0.1927
PS(127k)-PEO(1k)-PS(127k)	14.51	4.7	205.70	0.4552
PS(107k)-PEO(20k)-PS(107k)	2.13	21.3	146.90	0.2929
PS(305k)-PEO(20k)-PS(305k)	3.99	21.3	248.05	0.3942
PS(168k)-PEO(10k)-PS(168k)	4.26	15	195.98	0.3242
PS(1045k)-PEO(10k)-PS(1045k)	12.74	15	440.11	0.3492

Table 2 : Triblocks employed in this study and the interchain spacing compared to overlap spacing

Figure 3 shows that the grafting density of the symmetric to moderately symmetric triblocks scale with the reciprocal of the head size ($1/N_A$). For highly asymmetric triblocks, the surface density scales with the reciprocal of the square of the asymmetry ratio ($1/\beta^2$) as shown in Figure 4. Both of these results are consistent with the predictions of the scaling theory of Marques and Joanny for diblock adsorption. The B-A-B triblock materials are thus seen to behave the same as diblock materials as far as the effect of chain composition on the structure of the adsorbed layers is concerned.

Conclusions

It is seen from the (**D / D_{OVER}**) values in Table 2 that the B-A-B triblocks are stretched and hence it can be concluded that middle-adsorbing triblock materials can form a brush structure. Such materials should therefore be as effective as A-B diblock materials in steric stabilization applications.

It can be concluded that the middle-adsorbing triblock materials behave very similar to diblock materials. The change in composition of the B-A-B copolymers produces similar changes in the structure of the adsorbed layer as changes in the A-B diblock layer. The surface density for the symmetric to moderately symmetric triblocks scale with the reciprocal of the head size ($1/N_A$). For highly asymmetric triblocks, we find that the surface density scales with the reciprocal of the square of the asymmetry ratio ($1/\beta^2$) . The B-A-B architecture shares an important feature with the A-B diblock, namely attachment at a single location along the chain. This is

in contrast to the A-B-A architecture where the chains may attach at two different locations; this later case may produce distinctly different behavior.

References

1. Napper, D.H. *Polymeric Stabilization of Collodial Dispersions* (Academic Press, London, 1983).
2. Flory, P.J. *Principles of Polymer Chemistry* (Cornell University Press, Ithaca, NY, 1953).
3. Milner, S.T. *Science* **251**, 905-914 (1991).
4. Swalen, J.D., *et al. Langmuir* **3**, 932-950 (1987).
5. Marques, C. M.; Joanny, J. F. *Macromolecules*, **22**, 1454 (1989).
6. Guzonas, D.A., Boils, D., Tripp, C.P. & Hair, M.L. *Macromolecules* 25, 2434-2441 (1992).
7. Azzam, R.M. & Bashara, N.M. *Ellipsometry and Polarized Light* (North Holland Publication, Amsterdam, 1979).
8. Motschmann, H.; Stamm, M; Toprackcioglu, C. *Macromolecules*, **24**, 3681 (1991).
9. Pai-Panandiker, R. S.; Dorgan, J. R. *Reviews of Scientific Instruments*, **66**, 1121 (1995).
10. Uyanik, N; Baysal, B. M. *J. Appl. Poly. Sci.*, 41, 1981 (1990).
11. Dorgan, J. R.; Stamm, M.; Toprackcioglu, C. Macromolecules, **26**, 5321 (1993).

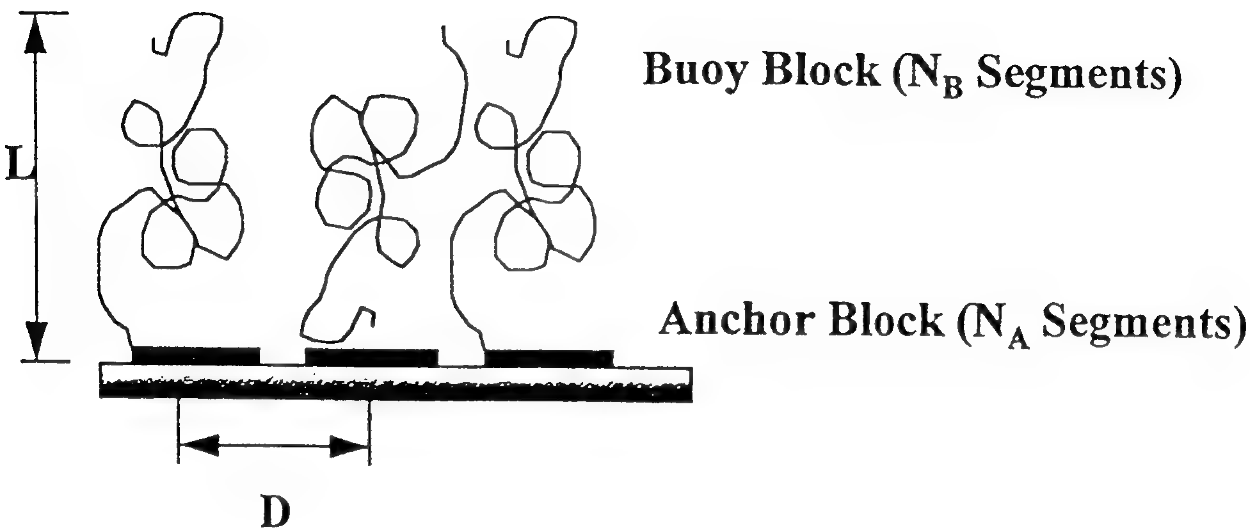

$$\boxed{\beta = a'\left(N_B / N_A\right)^{0.6}}$$

$$\boxed{\sigma = (1/D)^2}$$

Figure 1 : Schematic representation of physical parameters of block copolymer adsorption.

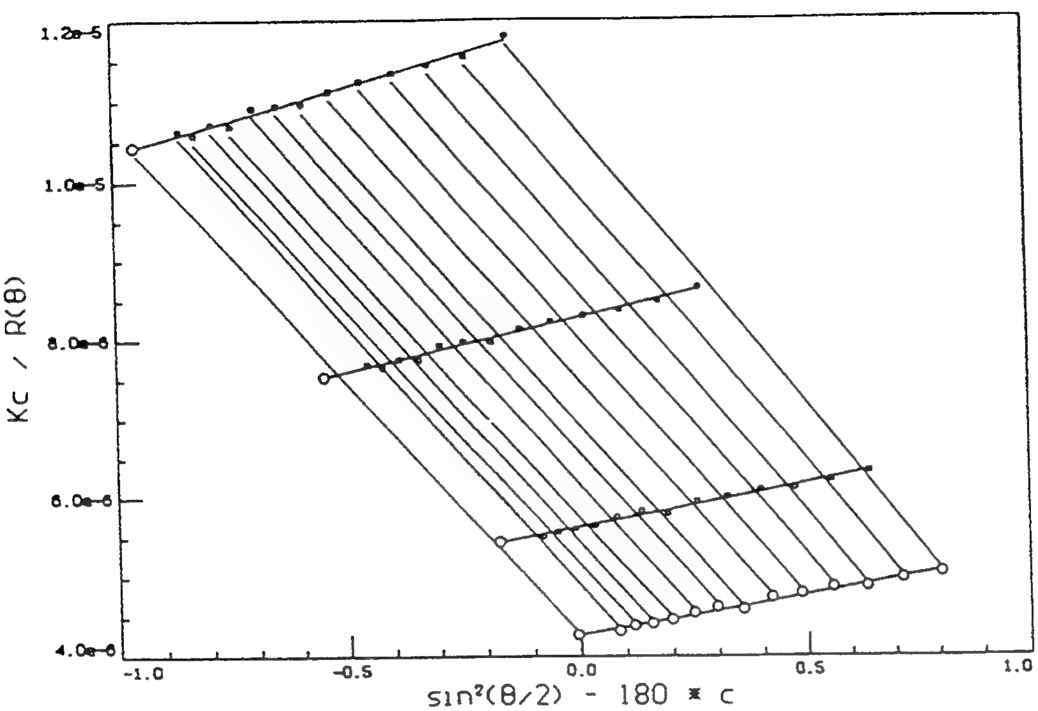

Figure 2 : Zimm plot for PS(107k)-PEO(20k)-PS(107k).

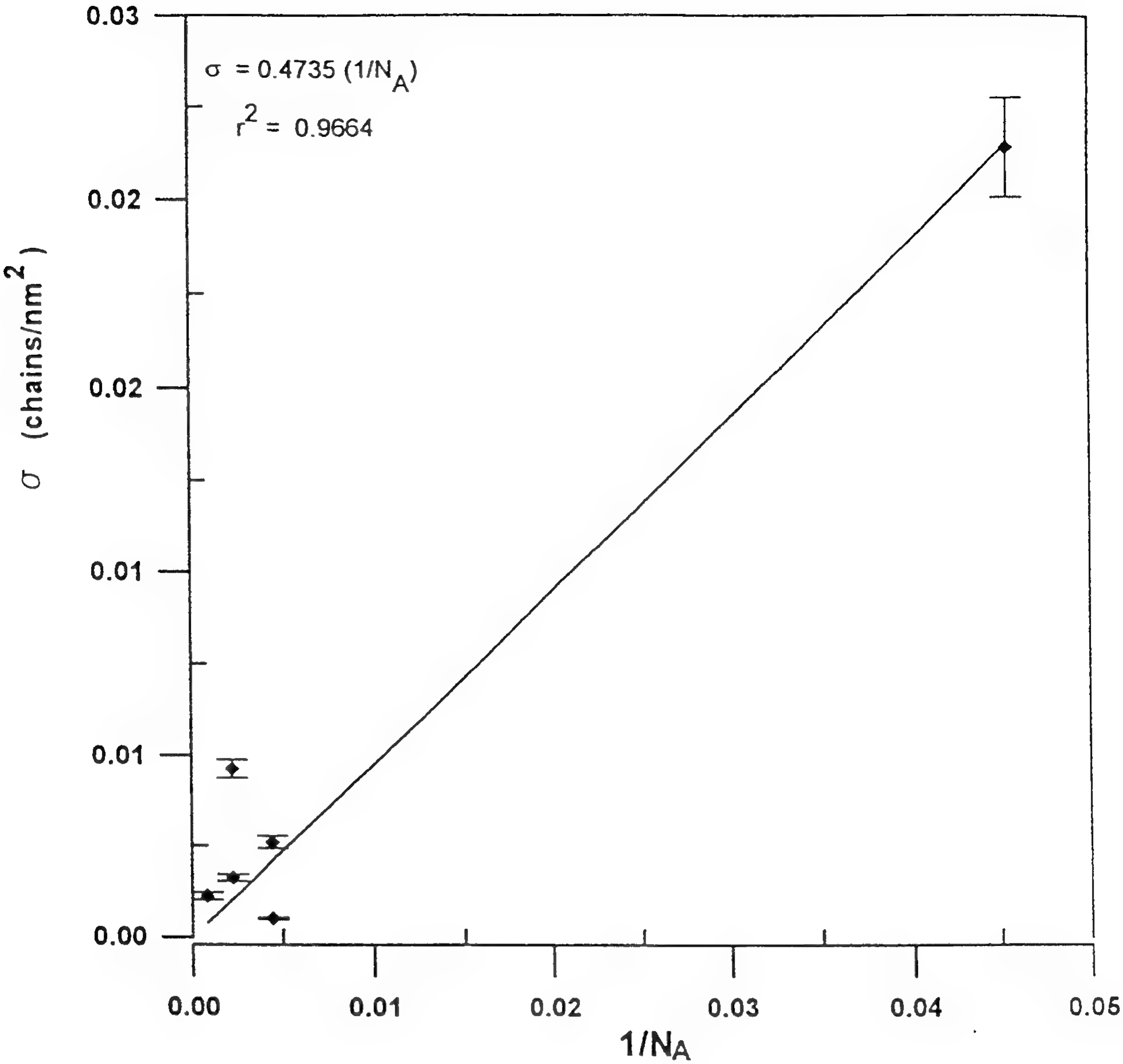

Figure 3 : Scaling behavior of symmetric to moderately symmetric triblocks

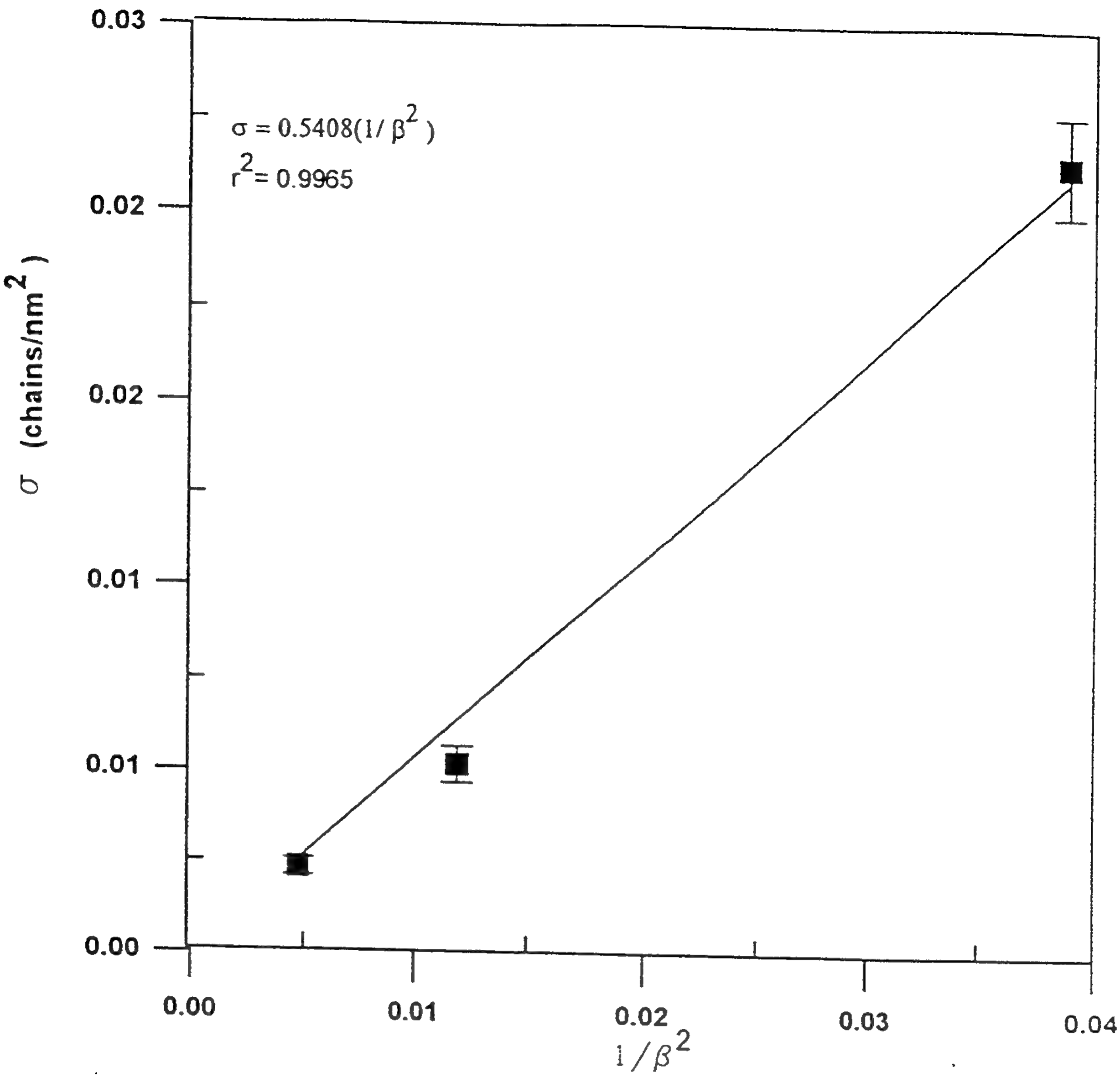

Figure 4 : Scaling behavior of highly asymmetric triblock copolymers.

Mary Ann Jungbauer report unavailable at time of publication.

STUDIES OF SECOND HARMONIC GENERATION IN GLASS WAVEGUIDES

David Statman
Associate Professor
Department of Physics and Department of Chemistry

Allegheny College
Meadville, PA 16335

Final Report for:
Summer Research Extension Program
F.J. Seiler Research Laboratory

Sponsored by:
Air Force Office of Scientific Research
Bolling Air Force Base, D.C.

and

F.J. Seiler Research Laboratory

December 1995

STUDIES OF SECOND HARMONIC GENERATION IN GLASS WAVEGUIDES

David Statman
Associate Professor
Department of Physics and Department of Chemistry
Allegheny College

ABSTRACT

Germanosilicate glass waveguides were electrically poled using interdigitated electrodes. This poling resulted in a quasi-phasematched second order susceptibility. Second harmonic light was observed. Measured intensities were one to two orders of magnitude smaller than expected based on previous electric field induced second harmonic (EFISH) generation studies with the same interdigitated electrodes. The dynamics of the EFISH signals were studied. Exponentially decaying signals suggest that through charge migration, via dielectric relaxation and electronic drift, a compromising field is established during the poling. This results in a weaker second order susceptibility.

STUDIES OF SECOND HARMONIC GENERATION IN GLASS WAVEGUIDES

David Statman

1. Introduction.

Second harmonic generation of laser light in germano-silicate glass fibers and waveguides is a well established phenomenon[1]. It has been suggested that glasses which macroscopically possess inversion symmetry, the third order susceptibility acts on an internal electric field. This results in the establishment of a second order susceptibility by which second harmonic generation can be accomplished[2]. While the mechanism of second harmonic generation via seeding is still a matter of investigation, current modeling is based on a photorefractive effect where a space charge field is established within the glass[3].

It has also been experimentally confirmed that second harmonic light can be generated in glasses via the application of an electric field. In fact, electric field induced second harmonic generation (EFISH) has been demonstrated in glass fibers[4], and planar glass waveguides[5]. By using interdigitated electrodes, Kashyar[4] demonstrated quasi-phasematched SHG in germanosilicate fibers, and Weitzman, Kester, and Osterberg[5] demonstrated quasi-phasematched SHG in germanosilicate planar waveguides. Their measured second harmonic signal varied as the square of the applied voltage across the electrodes, as expected from theory.

Because electric fields are capable of facilitating second harmonic generation in glasses, there has also been significant effort to electrically pole glasses. Myers, Mukherjee, and Brueck[6], as well as Nasu, et al.[7], demonstrated poling of bulk glass by applying between 1 kV and 5 kV across a glass sample at elevated temperatures. Each reported second order susceptibilities on the order of 1 pm/V. Bergot, et al[8] were successful in poling glass fibers by fabricating them with capillary electrodes on opposite sides of the core. By apply a dc electric field of 40 kV/cm, they were able to achieve a second order susceptibility of 3 fm/V. Bergot, et al. found that the second order susceptibility could be enhanced 20 times with CW excitation by Argon-laser light at 488 nm during the poling process[8]. In order to enhance the efficiency of second harmonic generation in optical fibers, Kazansky et al.[9] thermally poled with interdigitated

electrodes. The periodicity of the electrodes allowed for quasi-phasematching. By applying 4.3 kV across the electrodes, they were only able to obtain 20 pW of second harmonic for 200 mW of IR pump. This amounts to a second order susceptibility of about 5 fm/V, orders of magnitude less than expected. Suggesting that a source of electric field spreading was electric breakdown in air, they were able to improve the amount of generated second harmonic 40 fold by poling the fiber in a vacuum[10]. Okada, et al., were successful in corona poling glass waveguides[11]. They used a novel technique for phasematching by fabricating a wedge waveguide and finding the waveguide thickness where the TM_0 mode of the fundamental was phasematched to the TM_2 mode of the second harmonic. With 5 kV applied to a 2.8 micrometer thick waveguide, they achieved a second order susceptibility of 0.5 pm/V. Okada, et al. also found that between 100 and 300°C poling temperature had no effect. Nasu, et al.[7], however, found that they could not pole glass at temperatures below 100°C.

In order to understand the poling process better, Mukherjee, Myers, and Brueck[15] studied the dynamics of poling at different temperatures for the case of corona poling in bulk glass. They found that the poling and closed circuit depoling rates were characterized by a ~ 1 eV activation energy. For the open circuit depoling at elevated temperature, Mukherjee, et al. measured an activation energy of only 0.4 eV. They suggested that this was due to surface charge mobility rather than a bulk effect.

In this article, we investigate the effects of charge mobility on electric field induced second harmonic generation in waveguides, and discuss the impact that has on various poling schemes. By measuring the time dependence of EFISH, we show that charge migration results in a compromising electric field which mitigates poling in air using interdigitated electrodes. This results in smaller than desired second order susceptibilities, just as described by Kazansky. The experiment is presented in section 2. In section 3, a discussion of surface charge dynamics and its effect on the internal electric field is given. It is shown that such analysis agrees with the experimental data reasonably well.

2. Experiment.

Thermal Poling with Interdigitated Electrodes.

Planar germanosilicate waveguides which were nominally 2 micrometers in thickness on a glass substrate were poled at 200°C. Interdigitated electrodes of the type used by Weitzman, et al.[5] were placed on the top surface of the waveguide. The electrodes were never in direct contact with the glass. There was an air space of about a micrometer between the electrodes and the glass. The electrodes were spaced 9.5 micrometers apart. In order for the poled field to be quasi-phasematched to the TM_0 modes of the fundamental wavelength (1.064 micrometers) and the second harmonic (532 nm), the electrodes were oriented 31° with respect to the propagation axis of the fundamental. This angle was determined by measuring the propagation constants, β, of the fundamental and second harmonic in the waveguide via prism coupling[13]. Care was taken to make sure the waveguide and electrodes were clean. After heating the waveguide to 200°C in an oven, voltage was applied to the electrodes. In two runs 30 V were applied, in a third run 100 V were applied. The current was monitored throughout the poling process to be sure the resistance across the electrodes was never less than a megaohm. The temperature in the oven was maintained at 200°C for one hour. The waveguide was allowed to cool overnight with the voltage applied.

After poling, the waveguide was probed for SHG using a Q-switched mode locked Nd:YAG laser. The experimental setup is shown in Fig. 1. The waveguide was mounted in a prism coupler similar to one used by Ulrich and Torge[14]. The output from the laser was directed through a half wave plate and polarizer to insure that the waveguide modes were TM. The laser light was focused into the waveguide, and the waveguide was angle tuned so that the excited mode was TM_0. The prism coupler and waveguide were mounted on a tilt table. In this way, the angle of the propagating beam could be adjusted with respect to the grating vector of the poled field. The propagation length along the poled portion of the waveguide was about 1 cm. The coupled IR output was monitored with a detector. Typically the throughput of IR was 40%. This is consistent with a 1 dB loss in each of the coupling prisms, and a 2 dB loss along the length of the waveguide. For 240 mW average input IR power, the IR power in the waveguide varied from 190 mW down to 120 mW. The SHG signal was measured with a photomultiplier (PM) whose output was measured with a boxcar averager. The laser provided the trigger source. Before the PM were placed, filters to insure that no IR signal

was measured. In addition, a spike filter for wavelength 532 nm was introduced. This was to insure that the signal measured was SHG and not spurious fluorescence. The spike filter typically reduces the intensity of 532 nm light by about 50%. All signals were tested by comparing the signal with and without the filter. If the ratio was less than 50%, the signal was rejected as not being second harmonic.

For the two cases in which the waveguide was poled with 30 V applied, second harmonic signal was detected by the PM tube. On the most sensitive setting of the boxcar averager, second harmonic signal detected was well above the noise level. The signal to noise ratio exceeded 30. The measured intensities were about 50 to 100 picoWatts. The intensities were too low to be seen visibly. When the waveguide was poled with 100 V applied, it was expected that the measured intensity should increase tenfold. In this case, however, the input intensity was measured to be about 400 mW, giving waveguide IR powers from 300 mW down to 200 mW. This resulted in IR degradation of the waveguide before any intensity measurement could be made. However, before complete degradation of the waveguide, green light was seen visibly in the waveguide. This suggests that the green power was at least a nanoWatt.

The tilt angle of the poled electric field grating vector with respect to the input was varied to determine the SHG efficiency as a function of angle. It was found that the acceptance angle was about 3.4°, around the 31° angle that the poling field grating vector made with the fundamental at maximum SHG.

Maker fringe measurements were attempted on the poled waveguides. No signal was observed. This suggests that either $\chi^{(2)}$ is less than about 5 fm/V, the resolution of our instrumentation, or the quasi-phasematching of the poled field (in and out of the waveguide) along the length of the waveguide resulted in a cancelling out of SHG signal through destructive interference.

Dynamics of Electric Field Induced Second Harmonic (EFISH).

In a second set of experiments, the generated light was measured in order to compare SHG signal from an applied field to that of the poled waveguide. The measured EFISH signal was significantly larger than the measured SHG signal from the poled waveguide. It was also found, however, that the EFISH signal was not robust, i.e., it decayed. This suggested a possible explanation for the low SHG signals from the poled waveguide. In particular, if at room temperature a compromising field is established within the waveguide such that the internal field is much less than

the applied field, then it is also possible that such compromising field is also established at elevated temperatures. The poling field within the waveguide, then, may well be much less than intended. While Kazansky, et al.[10] attributes this diminution of poling field strength to electric field spreading from electric breakdown of air, we can use no such arguments. Our poling voltages never exceeded 100 V, as compared with Kazansky et al's 4300 V. In addition, we continually monitored the current during the poling process and saw no change. If there were any electric breakdown in air, it was certainly not across the electrodes. In the following set of experiments, the time dependence of the EFISH signal was measured in a second waveguide.

The experimental set-up was the same as that shown in Fig. 1. In addition, interdigitated electrodes were brought to the surface of the waveguide in a manner similar to Weitzman, et al[5]. The angle calculated between the electric field grating vector and the propagation direction was again based on the β's calculated from the coupling angles in prism coupling. In this case that angle was 15.5°. We found that the acceptance range was about 2.5°, and set the angle at that for the best measured EFISH signal. As in the poling process, the electrodes never actually touched the waveguide surface. Rather than turn the voltage across the electrodes on and off, the electrodes were moved on and off the waveguide. The propagation length for this waveguide was about 2 cm. This resulted in losses of 6 dB for the IR. The measured throughput was 25%. Using these numbers, along with the higher losses for green light, it was seen that the EFISH signals were more than ten times the signal measured from poling.

Fig 2 shows the time dependence of the SHG signal from the EFISH signal for five different trials when the applied voltage was 80V. Trials 3 and 5 show the EFISH signal when the field was applied. Trials 1, 2 and 4 show the SHG signal when the field was removed. What is obvious from these measurements is that the second harmonic signal decays over a period of a few minutes. After two hours no signal was present for either when the field was applied, or when it was removed. In previously conducted experiments[15], the EFISH signal also showed a decay, but did not appear to decay to zero. Rather, it appeared to come to some steady state value. Again, when the field was removed, the SHG signal did go up and then did decay to zero. Those particular EFISH measurements, however, did not explore longer time behavior. It is not clear whether there was a longer decay to zero. It is possible however that whether the EFISH signal decays to zero is dependent on factors not controlled during the experiment. In trials 3 and 4 the IR pump was not present between measurements. In trials 1, 2 and 5 the IR pump was always present. Clearly the IR fundamental

had no significant impact on these decays.

This decay demonstrates the dynamics of a compromising field being established during the EFISH experiment, and decaying away when the electrodes are removed. The presence of SHG, however transient, upon the removal of the electrodes is a confirmation of the establishment of that field. Without the field it decays with the same dynamics by which it was established.

In Fig. 3 the decaying SHG signal for when the electrodes were removed are shown for three different applied voltages: 60V, 80V and 100V. While the short time behavior appears to be voltage dependent, the longer tail appears to have the same slope for all three trials.

Whether the observed compromising field is due to the development of a surface space charge field, or the development of an internal space charge field is not clear from the data presented. What is clear from the data, however is that there is a fast decay, with a time constant τ_1, and a slow decay with a time constant τ_2. The fast decay is more than likely due to charge migration. It is not clear what the source of the slow decay is. In Figs. 4 and 5, the internal electric field (given by the square root of the second harmonic signal) is shown, and fit to an equation of the form (see appendix A).

(1)
$$\frac{E}{E_i} = \sqrt{\frac{I(2\omega)}{I(2\omega)_i}} = A\frac{e^{-\frac{t}{\tau_1}}}{1+b'\left(1-e^{-\frac{t}{\tau_1}}\right)} + (1-A)e^{-\frac{t}{\tau_2}}$$

Where E is the dc internal field within the waveguide. Table 1 gives the fit parameters. The first term of Eq. 1 is of the general form of a decay due to dielectric relaxation, electronic drift and diffusion, whereas as the second term is a simple exponential decay.

3. Discussion.

In general the complex amplitude of the second harmonic A_2 in a planar waveguide is given by[16]

(2)
$$\frac{dA_2}{dz} + \frac{\alpha}{2}A_2 = i\frac{2\pi\omega_2^2}{\beta_2 c^2} f(z)\chi^{(2)} A_1^2 e^{i\Delta\beta z}$$

where A_1 is the complex amplitude of the fundamental, z is the propagation direction, α is the attenuation coefficient due to linear losses, β_2 is the propagation constant in the waveguide, determined by the waveguiding mode, and f(z) accounts for the overlap integrals of the waveguiding modes.

Within the poled waveguide, $\chi^{(2)}$ is determined by the internal electric field through the third order susceptibility, $\chi^{(3)}$. This poled field changes the symmetry of the glass so that it no longer has a macroscopic inversion center thereby allowing second harmonic generation. Phase matching is accomplished with periodic poling using interdigitated electrodes. In our experiment, the poling field is given approximately by $E_0\sin(\Delta\beta z)$. If the poling process is efficient, $\chi^{(2)} \sim \chi^{(3)}E_0\sin(—\Delta\beta z)$. The second harmonic is phasematched with the fundamental.

Within the nondepleting pump approximation, Eq. 2 can be solved for the second harmonic field;

(3)
$$A_2 = \frac{2\pi\omega_2^2}{\alpha\beta_2 c^2} f(z)\chi^{(3)}E_0 A_1^2\left(1 - e^{-\frac{\alpha z}{2}}\right)$$

For glass waveguides the third order susceptibility is $\chi^{(3)} \approx 10^{-22}\ m^2/V^2$ and the linear attenuation for the second harmonic is approximately $\alpha = 0.46\ cm^{-1}$. For an applied field of 100V, a poled field $E_{DC} = 10\ V/\mu m$ is expected[16]. That suggests that $\chi^{(2)}$ should be approximately 1 fm/V. Clearly this is much smaller than other reported values of approximately 1 pm/V, where the applied or poling field is two orders of magnitude greater than that applied here. In order to achieve higher second order susceptibilities, larger voltages must be applied. With our setup, however, no more than 100 V could be applied. Otherwise, the electrodes would be damaged.

EFISH experiments suggest that even with this small value of $\chi^{(2)}$, the second harmonic power in the poled waveguide should be at least an order of magnitude greater than measured. However, these subnanoWatt powers are consistent with the experimental results of Bergot, et. al. [8] and Kazansky, et. al.[9] It would appear as though the poling process is not as efficient as one would like. For our experiments, the electric field spreading due to the breakdown of air cannot be invoked, since the applied field is only 100kV/cm. Our EFISH experiments suggest that one possible reason for this is the establishment of a compromising charge field.

Consider a current density being driven by the drift and diffusion of charge,

(4) $$\mathbf{j} = \mu\rho_c\mathbf{E} - D\nabla\rho_c$$

where the conductivity, σ is given by the product of the charge mobility, μ and the mobile or conductive charge density ρ_c; $\sigma = \mu\rho_c$. From continuity, the time dependence of the total charge density can be determined;

(5) $$\nabla \bullet j + \frac{\partial\rho}{\partial t} = 0$$

and hence, from Poisson's equation the time dependence of the internal electric field;

(6) $$\varepsilon\varepsilon_0 \nabla \bullet E = \rho$$

Eqs. 4 - 6 can be solved for an internal electric field having the form $E = E_0\sin(\Delta\beta x)$. Since the total charge density includes bound charges as well as conductive charges, from Eq. 6 it can be assumed that the conductive charge density has the form $\rho_c = \rho_{co} + \phi\varepsilon\varepsilon_0(\nabla \bullet E + \Delta\beta E_0)$, where ϕ is a dimensionless parameter corresponding to the amplitude of the conductive charge density modulated by the electric field. ρ_{co} is the background conductive charge density. If initially, at $t = 0$, the internal electric field (within the waveguide) is E_i with an amplitude E_{0i}, , then that field decays to zero as

(7) $$E = E_i \frac{e^{-\frac{t}{\tau_1}}}{1 + bE_{0i}\left(1 - e^{-\frac{t}{\tau_1}}\right)(1 + \cos\Delta\beta x)}$$

with

$$\tau_1 = \frac{1}{\frac{\mu\rho_{co}}{\varepsilon\varepsilon_0} + \phi D\Delta\beta^2}$$

and

$$b = \frac{\mu}{\frac{\mu\rho_{co}}{\phi\Delta\beta\varepsilon\varepsilon_0} + D\Delta\beta}$$

The diffusion coefficient, D, of a charge is typically given by the Einstein relation $D = \mu k_B T/e$. b is then given by

$$b = \frac{e}{\frac{e\rho_\infty}{\phi\Delta\beta\varepsilon\varepsilon_0} + k_B T\Delta\beta}$$

Eq. 7 can be compared to the first term in the empirical expression given by Eq. 1.

It is clear from Eq. 7 that spatially harmonic electric fields are generated during the decay of the internal field. The phase matched component of the internal field, then is given by the first term in Eq. 1 where b' is approximately equal to bE_{0i}. For fields on the order of 10V/μm with $\Delta\beta = 2\pi/\Lambda = 3.3 \times 10^5$ m^{-1}, the product bE_{0i} can be as high as 1.2 $\times 10^3$ when ϕ is very large (much greater than unity). Diffusion and drift dominate the decay of the field. For $\phi = 0$ the product bE_{0i} equals 0 and dielectric relaxation dominates the decay of the field. In both cases, large bE_o and small bE_o, the internal electric field decays to zero via charge migration.

For glass the conductivity $\sigma \approx 1 \times 10^{-12}$/ohm-m. Assuming the dielectric relaxation time is much smaller than the diffusion time, τ_1 is approximately equal to the dielectric relaxation time. Given that the dielectric relaxation time is $\tau_{di} = \varepsilon\varepsilon_0/\sigma$, τ_1 is expected to be about 35 s. It is encouraging that while the spread of fit values for τ_1 is not small, its mean is about 35 s. The expected and measured values of τ_1 are certainly within an order of magnitude of each other. The mobility, μ, and the conductive charge density ρ_∞ cannot be calculated independent of ϕ. Nevertheless, for a mean value of $b' = bE_{0i} = 5$ our measurements give $\mu\phi = b/\tau_1\Delta\beta = 4.3 \times 10^{-14}$m^2/Vs, and $\rho_\infty/\phi = \varepsilon\varepsilon_0\Delta\beta/b = 24$ C/m^2. Assuming ϕ to be on the order of unity (meaning that the compromising space charge field is mostly due to conducting charges and not bound charges) this gives a charge mobility of 4.3×10^{-14} m^2/Vs and a conductive charge density of 24 C/m^2. This charge density corresponds to a carrier density of 1.5×10^{20}/m^3. These values are within an order of magnitude of the expected values for charge mobility and carrier density in glass. Our results, then, suggest that the compromising field is established via dielectric relaxation and electronic drift. Diffusion, however, is insignificant since it is a much slower process and the charge modulation is not expected to be large.

4. Conclusions

We report the observation of second harmonic generation in poled glass waveguides. Measured intensities, however, were at least an order of magnitude less than expected. From EFISH measurements it was seen that when an electric field is applied to the waveguide, the internal field decays in a way that is multiexponential. We suggest that this decay is the result of charge migration through dielectric relaxation and electronic drift. Diffusion is not considered to be significant. This charge migration establishes a compromising electric field, which opposes, at least partially, the applied field.

In the process of poling the waveguide, if these compromising fields are established, then the poling field can be orders of magnitude less than that applied. The result is a much lower second order susceptibility, hence much lower second harmonic conversion efficiency. It appears as though as long as there are enough conductive charges available to create the compromising field, poling will be inefficient. This would suggest that poling fields must exceed $\rho_c/\Delta\beta\varepsilon\varepsilon_0$, $E_0 > \rho_c/\Delta\beta\varepsilon\varepsilon_0$ by an order of magnitude or more. Assuming ρ_c to be between 10 and 100 C/m^3, the poling field, then, must be greater than 10^7 V/m by an order of magnitude or more. While it cannot be determined from these experiments whether the charge migration is surface or bulk, surface charge effects can be mitigated if the poling is done in a vacuum, as Kazansky has done.

Appendix A:

In the experimental section, the decay of the internal electric field was fit to Eq. 1. This equation was based on the assumption that the dynamics of that component of the electric field due to charge migration (as opposed to dipole relaxation) are determined by drift and diffusion. Because the conductivity is dependent on the charge density, hence on the internal electric field, the drift term is proportional to the electric field; $\sigma E = aE^2$. A simplified form of this can be given as;

(A-1)

$$\frac{dE}{dt} = -aE^2 - \frac{1}{\tau_1}E$$

The first term in Eq. A-1 is due to drift, and the second term due to dielectric relaxation and diffusion. This can be solved to give

(A-2)
$$\frac{E}{E_i} = \frac{e^{-\frac{t}{\tau_1}}}{1 + aE_0\tau_1\left(1 - e^{-\frac{t}{\tau_1}}\right)}$$

which is Eq. 1, where $b = aE_0\tau_1$. A more rigorous derivation of the electric field dynamics can be found in Section 3.

References.

1. U. Osterberg and W. Margulis, Opt. Lett., **11**, 516 (1986), J. J. Kester, P.J. Wolf, and W.R. White, Opt. Lett., **17**, 1779 (1992).

2. R. H. Stolen and H.W.K. Tom, Opt. Lett., **12**, 587 (1987).

3. D.Z. Anderson, V. Mizrahi, and J.E. Sipe, Opt. Lett., **16**, 796 (1991).

4. R. Kashyar, J. Opt. Soc. Am., B, **6**, 313 (1981).

5. P.S. Weitzman, J.J. Kester, and U. Osterberg, Electron. Lett., **30**, 697 (1994).

6. R.A. Myers, N. Mukhergee, S.R.J. Brueck, Opt. Lett., **16**, 1732 (1991).

7. H. Nasu, H. Okamoto, K. Kurachi, J. Matsuoka, K. Kamiya, A. Mito, and H. Hosono, J. Opt. Soc. Am.,B, **12**, 644 (1995).

8. M.V. Bergot, M.C. Farries, M.E. Fermann, L.Li, L.J. Poyntz-Wright, P.St.J. Russell, and A. Smithson, Opt. Lett., **13**, 592 (1988).

9. P.G. Kazansky, A.Kamal, and P.St.J. Russell, Opt. Lett., **18**, 114 (1993).

10. P.G. Kazansky, V. Pruneri, and P. St.J. Russell, Opt. Lett. **20**, 843 (1995).

11. A. Okada, K.J. Shu, K. Mito, and K. Sasaki, Appl. Phys. Lett., **60**, 2853 (1992).

12. N. Mukhergee, R.A. Myers, and S.R.J. Brueck, J. Opt. Soc. Am.,B, **11**, 665 (1994).

13. J. Seligson, Appl. Opt., **26**, 2609 (1987).

14. R. Ulrich and R. Torge, Appl. Opt., **12**, 2901 (1973).

15. D. Statman and J.J. Kester, *private communication.*

16. R. W. Boyd, *Nonlinear Optics*, Academic Press, San Diego. 1992.

Table I. Fitting parameters to Eq. 1 (see text)

Trial	A	τ_1(s)	b'	τ_b(s)
1.	0.43	62	4.2	1200
2.	0.58	14	~0	233
3.	0.46	22	1.6	250
4.	0.48	37	8.5	180
5.	0.56	43	3.7	210

Figure Captions:

Fig. 1. Experimental set-up for waveguiding and second harmonic generation.

Fig. 2. SHG versus time: Trials 1 - 5. The applied voltage was 80 V. Trials 3 and 5 show the EFISH signal when the field was applied, trials 1,2, and 4 show the EFISH signal after the field had been removed.

Fig. 3. SHG versus time after removal of electric field, for V = 100V, 80V, and 60V.

Fig. 4. Internal electric field (normalized) versus time for the application of 80 V.

Fig. 5. Internal electric field (normalized) versus time for the removal of 80 V.

Fig 1

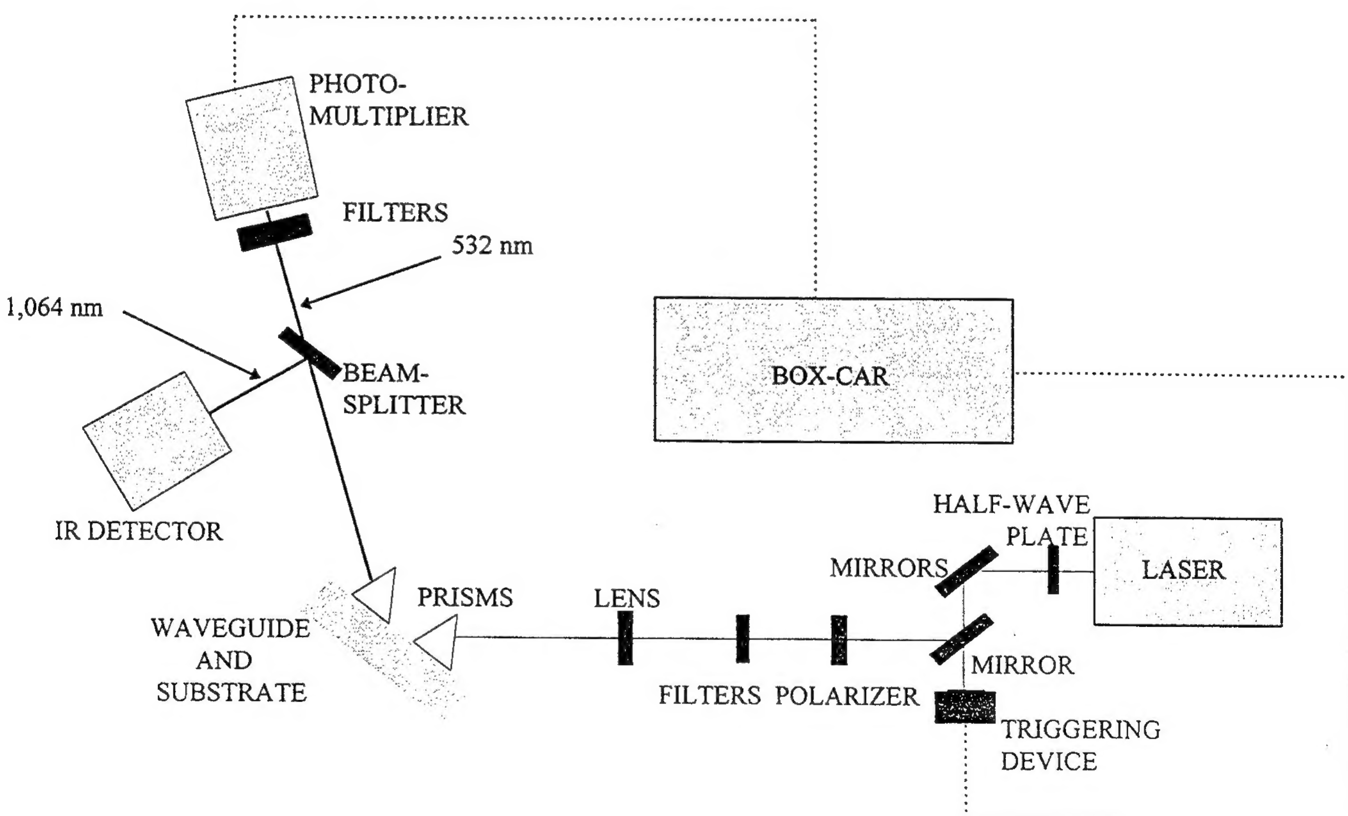
PHOTO-
MULTIPLIER
FILTERS
532 nm
1,064 nm
BEAM-
SPLITTER
BOX-CAR
IR DETECTOR
HALF-WAVE
PLATE
MIRRORS
LASER
PRISMS
LENS
WAVEGUIDE
AND
SUBSTRATE
MIRROR
FILTERS
POLARIZER
TRIGGERING
DEVICE

Fig 2.

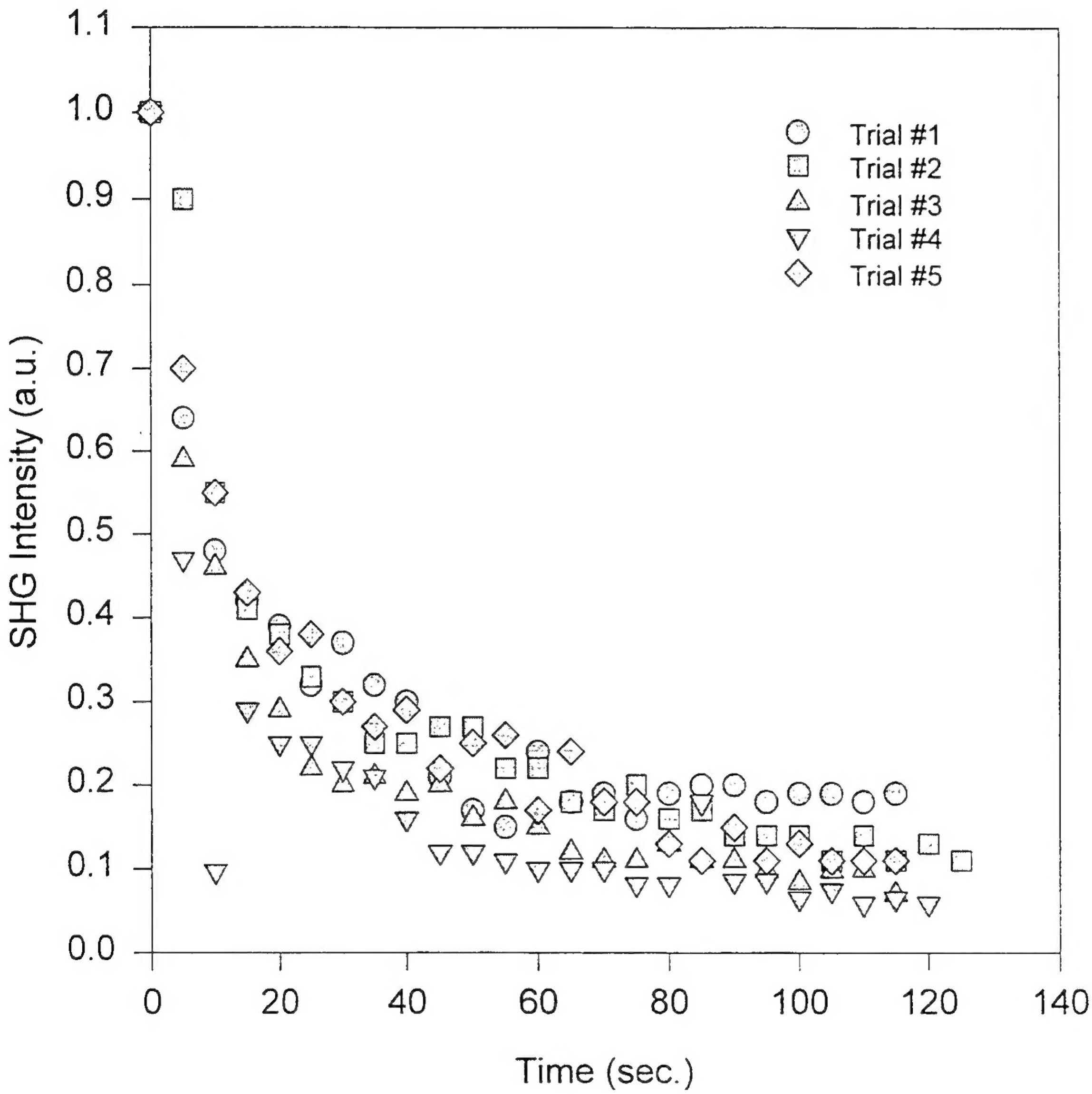

1.1
1.0
0.9
0.8
0.7
0.6
0.5
0.4
0.3
0.2
0.1
0.0
SHG Intensity (a.u.)
0
20
40
60
80
100
120
140
Time (sec.)
Trial #1
Trial #2
Trial #3
Trial #4
Trial #5